Catena 149 (2017) 742–759

Contents lists available at ScienceDirect

Catena

journal homepage: www.elsevier.com/locate/catena

# Use of airborne LiDAR and historical aerial photos for characterising the history of braided river floodplain morphology and vegetation responses

S. Lallias-Tacon [a,b], F. Liébault [a,*], H. Piégay [b]

[a] Université Grenoble Alpes, Irstea Grenoble, UR ETNA Erosion Torrentielle Neige et Avalanches, F-38402 St-Martin-d'Hères, France
[b] Université de Lyon, CNRS-UMR 5600 EVS, ENS, Lyon, France

ARTICLE INFO

*Article history:*
Received 12 May 2015
Received in revised form 6 July 2016
Accepted 21 July 2016
Available online 2 August 2016

*Keywords:*
Airborne LiDAR
Historical aerial photos
Braided rivers
Floodplain vegetation
Channel incision
Flood

ABSTRACT

This paper combines synoptic airborne LiDAR data with historical aerial photos to reconstruct floodplain formation and relate this with vegetation patch characteristics on three different alpine braided rivers in France displaying a gradient of geomorphic activity (Bouinenc < Drôme < Bès). LiDAR data were processed to extract understory topography and vegetation properties. Once combined with sequential aerial photographs for the dating of floodplain formation, they were used to establish the timing of channel incision associated with active channel narrowing. It has thus been possible not only to reconstruct the main incision periods following the end of the Little Ice Age, but also to show the geomorphic effect of floods on active channel widening, which was clearly modulated by sediment supply conditions. Well-developed floodplains with a predominance of mature vegetation units are associated with long-term narrowing and incision trajectories, whereas rivers maintaining a wide active channel over time show equi-diversity of floodplain vegetation units. The presence of shrub patches seems to be a good indicator of incision periods. A discriminant analysis using LiDAR-derived topographic and vegetation properties of floodplain patches as well as their age provided a validation of the expert-based mapping of physiognomic vegetation units (shrubland, sparse pioneer, dense pioneer, and post-pioneer units). This approach also provides insights into identification and interpretation of misclassifications and open new perspectives for exploring landscape ecological trajectories and their controlling factors.



## 1. Introduction

Knowledge of past trajectories of channel changes and associated riparian vegetation responses are fundamental for the understanding of floodplain landscape construction and composition, later used to define river management and restoration projects (Wallick et al., 2008; Zanoni et al., 2008; Dufour and Piégay, 2009; Downs et al., 2013; Bollati et al., 2014).

Studies of long-term channel adjustments are generally conducted with multitemporal analyses of aerial photographs and historical maps (Geerling et al., 2006; Ollero, 2010; Segura-Beltrán and Sanchis-Ibor, 2013; Bollati et al., 2014; Arnaud et al., 2015; Clerici et al., 2015; Dufour et al., 2015, see Table 1 for more details). Field data are occasionally used to improve reconstructions from historical documents, including topographic surveys (Segura-Beltrán and Sanchis-Ibor, 2013; Bollati et al., 2014; Arnaud et al., 2015; Clerici et al., 2015; Dufour et al., 2015) and dating from dendrochronological records (Stella et al., 2013; Bollati et al., 2014). These methods provide a good understanding of planimetric channel changes associated with natural events and human factors. However, the relation between planimetric changes and bed-level adjustment are rarely explored or present a certain number of difficulties. In fact, historical topographic surveys are rarely available or have only a low temporal frequency (Bollati et al., 2014; Arnaud et al., 2015). The understanding of vegetation dynamics has often been limited by photointerpretation when attempting to identify changing vegetation types over time (Miller et al., 1995; Geerling et al., 2006; Greco et al., 2007; Arnaud et al., 2015; Dufour et al., 2015, see Table 1 for more details), insufficient for a comprehensive analysis of vegetation responses. It is therefore common to collect field data on vegetation properties (species composition, density, height), but these are often limited to discrete spatial units such as transects or quadrats (Pautou and Girel, 1986; Gurnell et al., 2001; Kondolf et al., 2007; Dufour and Piégay, 2010).

Today, airborne light detection and ranging (LiDAR) data can be used to measure understory topography and vegetation properties along river reaches several kilometres long, with high altimetric precision. Recent studies have explored airborne LiDAR data to describe riparian forests (Farid et al., 2006; Hall et al., 2009; Johansen et al., 2010; Michez et al., 2013; Picco et al., 2014). These studies characterised

* Corresponding author at: Irstea Grenoble, UR ETNA Erosion Torrentielle Neige et Avalanches, 2 rue de la Papeterie-BP 76, F-38402 St-Martin-d'Hères, France.
*E-mail addresses:* sandrinelallias@yahoo.fr (S. Lallias-Tacon), frederic.liebault@irstea.fr (F. Liébault), herve.piegay@ens-lyon.fr (H. Piégay).

http://dx.doi.org/10.1016/j.catena.2016.07.038
0341-8162/

**Table 1**
Compilation of studies on floodplain changes and floodplain vegetation.

| References | River (study length) | Data | Planform changes | Bed level evolution | Floodplain | | Riparian forest | | |
|---|---|---|---|---|---|---|---|---|---|
| | | | | | Age | Topography | Extent | Units mapping | Characteristics |
| Ollero, 2010 | Ebro (Esp), 346 km | 8 series of aerial photos (1927–2004) | ✓ | | | | | | |
| Segura-Beltrán and Sanchis-Ibor, 2013 | The Rambla de Cervera (Esp) | 5 series of aerial photos (1946–2006) | ✓ | | | | | | |
| | | dGPS survey (2011, 10 km) | | ✓ | | | | | |
| Clerici et al., 2015 | Taro (Ita), 54 km | 9 series of maps and aerial photos (1828–2011) | ✓ | | | | | | |
| | | Cross-sections (1984) | | ✓ | | | | | |
| Bollati et al., 2014 | Trebbia (Ita), 22 km | Map (1885) and series of aerial photos (1954–2010) | ✓ | | | | | | |
| | | 4 series of cross-sections (1974–2009) + field check | | ✓ | | | | | |
| | | Dendrochronology | | ✓ | | | | | |
| Arnaud et al., 2015 | Rhin (Fra, Deu), 30 km | 8 series of aerial photos (1946–2008) | ✓ | | ✓ | | ✓ | | |
| | | 3 series of cross-sections (1950–2009) | | ✓ | | | | | |
| Geerling et al., 2006 | Allier (Fr), 6 km | 7 series of aerial photos (1954–2000) | | | ✓ | | ✓ | ✓ | |
| Greco et al., 2007 | Sacramento (USA) | 15 series of maps and aerial photos (1870–1997) | | | ✓ | | | ✓ | ✓ |
| Dufour et al., 2015 | Magra (Ita), 9.5 km and 10 km | 8 series of aerial photos (1937–2006) | ✓ | | ✓ | | ✓ | ✓ | |
| | | Vegetation cross-section (2006) | | ✓ | | | | | ✓ |
| | | Series of long profiles (1914–2000;1914–2006) | | ✓ | | | | | |
| | | Topographic cross-sections (2006) | | ✓ | | | | | |
| Miller et al., 1995 | North Platte (USA) | 2 series of aerial photos (1937–1990) + field check | | | | | ✓ | ✓ | |
| Farid et al., 2006 | San Pedro (USA) | LiDAR + field checks | | | | | | | ✓ |
| Michez et al., 2013 | Houille (Fra/Bel), 24 km | LiDAR | | | | | ✓ | | ✓ |
| Bertoldi et al., 2011 | Tagliamento (Ita), 21 km | LiDAR | | | | ✓ | | | |
| | | Aerial photo + field checks | | | | ✓ | ✓ | ✓ | ✓ |
| This study | Drôme, 5 km; Bès, 7 km; Bouinenc, 3 km (Fra) | LiDAR (2010) | | ✓ | | ✓ | | | ✓ |
| | | 8/9 series of aerial photos (1948–2006) | ✓ | | ✓ | | ✓ | ✓ | |

vegetation patches (e.g. extent, longitudinal continuity, height, density, and overhanging characteristics) based on the Canopy Height Model (CHM). On the Tagliamento River (Italy), Bertoldi et al. (2011, 2013) explored combined data from airborne LiDAR, colour air photographs and ground measurements to (1) study the colonisation pattern of exposed river sediments by riparian trees and its impact on channel topography (Bertoldi et al., 2011) and (2) investigate wood recruitment and deposition dynamics (Bertoldi et al., 2013). No studies have yet explored the capacity of LiDAR technology to quantify floodplain changes and associated vegetation patterns (Table 1).

French alpine valleys provide a good opportunity to study floodplain changes. Studies conducted here have highlighted that grazing abandonment in valley floors combined with a decrease in sediment supply during the 20th century have been efficient drivers of floodplain construction, combining channel incision and narrowing (Liébault and Piégay, 2002; Kondolf et al., 2007; Piégay et al., 2009).

Incision is usually measured using historical long profiles and it is often difficult to have >2 or 3 dates over the 20th century to describe it so that potential changing points are not always easy to detect whereas it is critical for linking channel changes and their potential drivers. In such context, the following approach may provide potentially more dates to characterize trend in channel changes and improve detection and dating of changing points. Associated changes in vegetation characters can also provide additional information on this trend in term of magnitude of change (e.g., major changes in vegetation mosaics) and landscape quality (e.g., patch diversity). Moreover, such approach which can be easily applied on a set of reaches and more ideally on a wide regional stream network is also a way of approaching large scale generalisation of observed changes, both being valuable for research purposes and application perspectives related to sediment management. Approached explored by Michez et al. (2013) and Demarchi et al. (2016) provide methodological background to move forward in this direction.

Such approach may be also useful to explore the theory of mutual interactions between riparian vegetation and hydromorphological drivers as stated by Corenblit et al. (2011) in a wider temporal perspective, considering simultaneously vegetation patch dynamics and channel changes so that practical, methodological and theoretical feedbacks are potentially expected.

This paper proposes new approaches to reconstruct floodplain formation and relate this to vegetation patch characteristics by combining information from sequential aerial photographs and airborne LiDAR data. The specific aims of this study were to explore new contributions of LiDAR in terms of (i) long-term channel adjustments, in particular the relation between incision and narrowing and (ii) vegetation characterisation, to explore the connection between long-term channel adjustment and vegetation response. A gradient of geomorphic activity was explored by means of three braided reaches displaying contrasting morphological trajectories since the late 1940s.

## 2. Study site

This study investigated three different sites in South-East France: the upper Drôme River between the Luc-en-Diois and Recoubeau-Jansac bridges, and the downstream parts of the Bès River and the Bouinenc Torrent, two tributaries of the Bléone River (Fig. 1A). These study

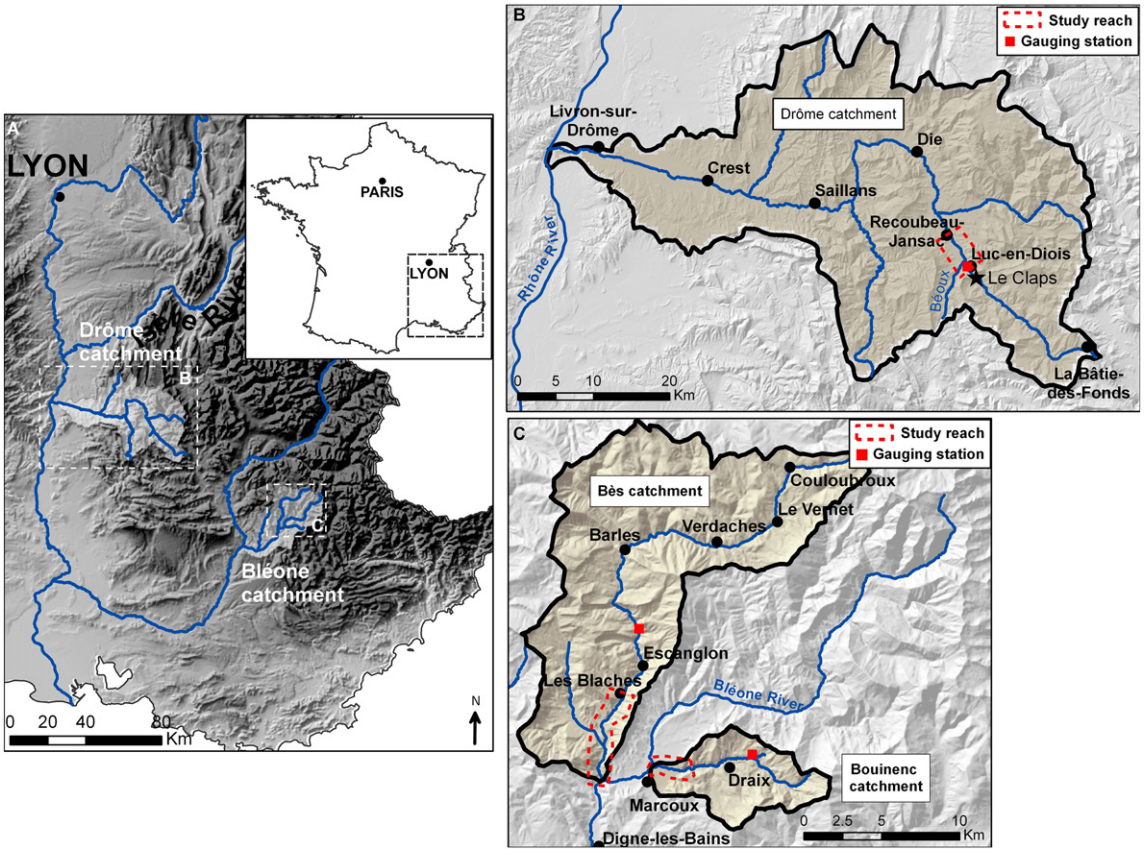


**Fig. 1.** Study sites: (A) location in SE France; (B) general map of the Drôme catchment with the position of the study reach; (C) general map of the Bès and the Bouinenc catchments with the position of the study reaches.

reaches were selected based on reported reconstructions of channel changes, as well as preliminary inspections of historical aerial photographs revealing a gradient of morphological trajectories since the late 1940s.

The upper Drôme is known as an incised river reach under the effect of intensive gravel mining in the 1970s and 1980s (Landon et al., 1998; Kondolf et al., 2002; Toone et al., 2014). The 5-km study reach (midpoint at 44°38′17.15″ N, 5°25′59.85″ E) is characterised by alternating straight single-thread and braided sections. The reach drains a 225-km$^2$ catchment, presents a mean channel slope of 0.01, an active width between 10 and 200 m, and no significant bank protections. It is mainly supplied by coarse sediment by the Béoux Torrent, which joins the Drôme 200 m upstream of the study reach.

The floodplain supports an extensive riparian forest that has developed since the 1950s. It is dominated by poplars (*Populus nigra*), willows (*Salix alba*), ash (*Fraxinus excelsior*), and alders (*Alnus glutinosa*) (Piégay and Landon, 1997; Gagnage, 2008). Poplars currently display local evidence of severe crown dieback (Gagnage, 2008; Dunford et al., 2009; Stella et al., 2013). Significant poplar growth declines coincided with the beginning of intensive gravel mining activity in the early 1970s (Stella et al., 2013).

Discharge has been recorded at the Luc-en-Diois gauging station since 1907. This station is located approximately 800 m upstream of the study reach. The hydrological regime reflects the influence of both snowmelt and the Mediterranean conditions (dry summer and autumn storms), with floods occurring in spring and fall. Between 1948 and 2010, two major floods occurred in January 1994 and December 2003, with 100- and 45-year return periods, respectively, and several medium floods ($Q_{10} > Q < Q_{50}$) occurred with the largest in 1951 and 1978 with 16- and 17-year return periods, respectively (Toone et al., 2014) (Fig. 2A). Flood activity has shown a long-term, overall decrease since 1850, with an abrupt, rapid reduction in the number of flood days per decade between approximately 1950 and 2002 (Landon et al., 1998; Liébault, 2003).

The Bès River is the main tributary to the Bléone River located near Digne-les-Bains. The study reach covers the last 7 km of the Bès River (midpoint at 44°09′32.89″ N, 6°14′36.49″ E). Here, the Bès is braided with a channel slope of 0.014 and a mean active channel width of 130 m. A recent study showed aggradation conditions upstream from the study reach (Liébault et al., 2013). Preliminary inspection of historical photos showed persistence of a wide active channel since the late 1940s, suggesting a sustained high sediment supply. Vegetated patches located in the river channel are mainly composed of poplars (*Populus spp.*), alders (*Alnus glutinosa*), ash (*Fraxinus excelsior*), willows (*Salix herbacea*), elms (*Ulmus glabra*) and shrubs (*Rubus* spp., *Juncus* spp.) (Navratil et al., 2010).

The flow record has been available since 1963 at the Pérouré gauging station approximately 1.5 km upstream of the study reach. The hydrological regime is characterised by spring snowmelt high flows, summer low flows, and rainfall autumn high flows. The mean annual discharge is 2.78 m$^3$ s$^{-1}$. Between 1963 and 2010, two major floods ($Q > Q_{50}$) occurred in February 1977 and January 1979 (two successive days), and two medium floods ($Q_{10} > Q < Q_{50}$) occurred in 1963 and 2009 (Fig. 2B).

The Bouinenc Torrent is a tributary to the Bléone River, near Digne-les-Bains (Fig. 1C). Substantial reforestation is observed on the Bouinenc catchment due to both torrent-control works and rural depopulation since the end of the 19th century (Vallauri and Vincent, 1999). Strong active channel narrowing is observed on historical aerial photos. The study reach corresponds to the last 3 km of the torrent, where the

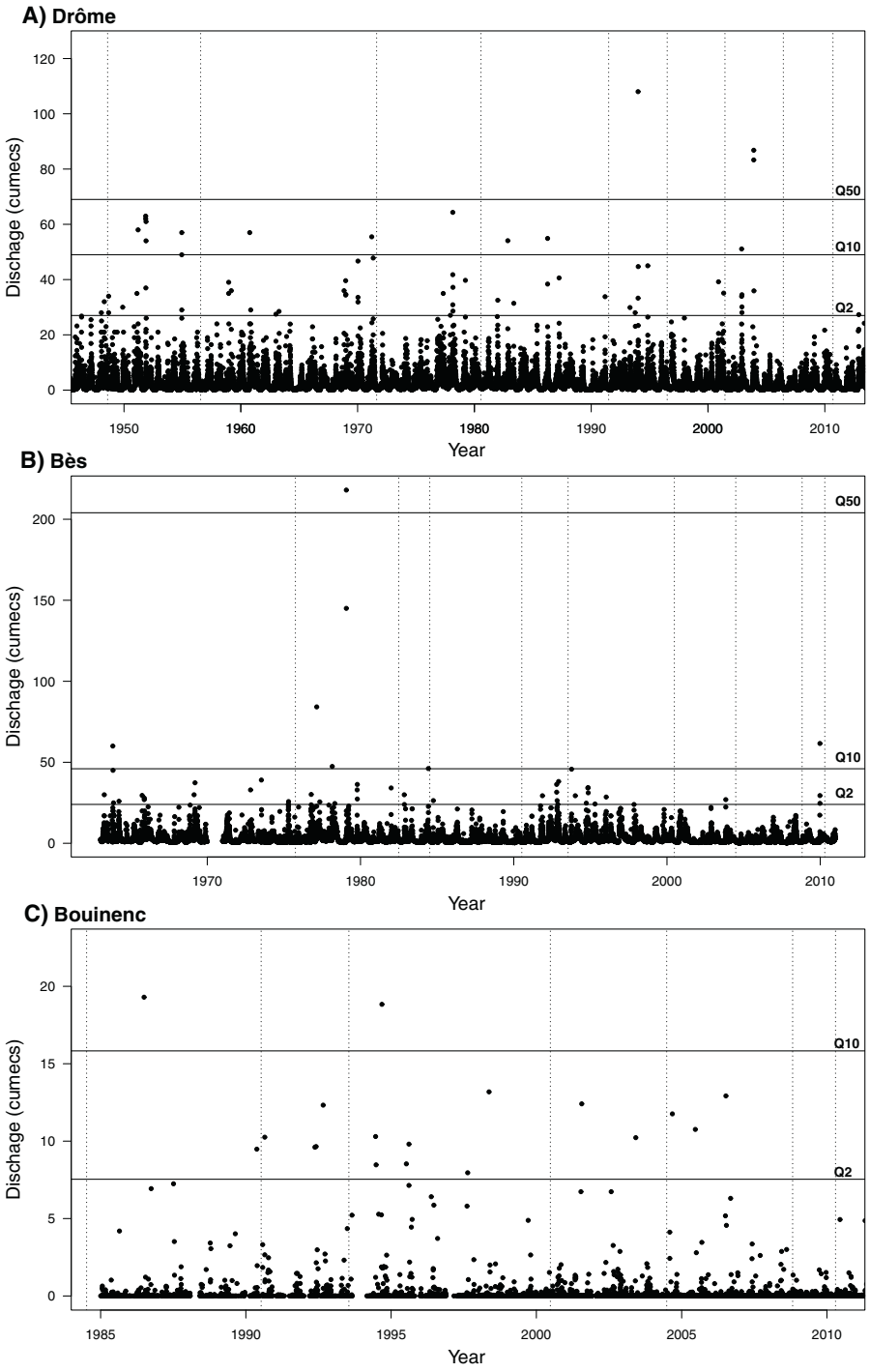


**Fig. 2.** (A) Mean daily discharge series of the Drôme River between 1948 and 2010 at Luc-en-Diois; data from the Luc-en-Diois gauging station (DREAL Rhône-Alpes); (B) the Bès River between 1963 and 2010 at Pérouré; data from the Pérouré gauging station (DREAL PACA); (C) maximum daily discharge series of the Laval Torrent (tributary of the upper Bouinenc Torrent) between 1983 and 2010; data from the ORE Draix-Bléone gauging station; dotted vertical lines correspond to the date of aerial photographs; solid horizontal lines correspond to the discharge of 2-, 10- and 50-year return period floods.

Bouinenc develops a wandering pattern in a 200-m-wide floodplain. The overall channel slope is 0.016 and the mean active channel width is 24 m (range: 10–45 m). The floodplain supports an extensive riparian forest.

The discharge of the Bouinenc has only been recorded since 2008 by Irstea, but a gauging station of the ORE Draix-Bléone observatory has been present on the Laval (0.86 $km^2$), a tributary of the upper Bouinenc, since 1983. Two medium floods ($Q_{10} > Q < Q_{50}$) occurred in 1986 and in 1994 in the Laval (Fig. 2C). A historical database recording natural hazard events (BD-RTM) reports damaging floods for the Bouinenc Torrent in September 1962 and 1986.

## 3. Methodology

The general framework used to characterize the history of the floodplain morphology and vegetation responses is based on a new approach that combines airborne LiDAR data and historical aerial photographs.

**Table 2**
Technical specifications of airborne LiDAR surveys; the altimetric and planimetric errors were provided by private companies from RTK-GPS ground control points locally measured on a road. SDE: standard deviation of error; NA: not available.

| | Bès\Bouinenc | Drôme |
|---|---|---|
| Device | Riegl LMS Q560 | Riegl VQ-480 |
| Date | 19/04/2010 | 13-14/09/2010 |
| Elevation precision of laser points (SDE in cm) | 5.0 | 5.2 |
| Planimetric precision of laser points (SDE in cm) | 15.0 | NA |
| Ground point density (points $m^{-2}$) | 6.4 | 3.5 |

### 3.1. Data acquisition and pre-processing

#### 3.1.1. Airborne LiDAR data

LiDAR surveys were collected by private companies, Helimap on the Drôme River and Sintegra on the Bès River and Bouinenc Torrent. Technical specifications of airborne LiDAR surveys are described in Table 2. The LiDAR returns were classified as ground and no ground points by data providers. Digital Terrain Models (DTMs) of 1-m resolution were derived from ground point clouds by triangulation and linear interpolation.

Digital Surface Models (DSMs) were extracted from the highest return point in 1-m pixel. For the Drôme River, the DSM presents many holes that were corrected using a 3 × 3-m median filter and by selection of the maximum value between the DSM and the filtered DSM. Canopy Height Model (CHM) rasters (pixel size, 1 m) were produced by subtracting the DTM from the DSM (Fig. 3A).

Detrended DEMs were constructed by removing the valley slope with a MATLAB script specifically developed for this purpose. First, the valley floor mean elevation is extracted for 1-m reaches, perpendicular to the river centerline. Then a long profile is derived and high frequencies are filtered. Finally, the mean elevation derived from the long profile is subtracted for each DEM pixel of the valley floor (Fig. 4).

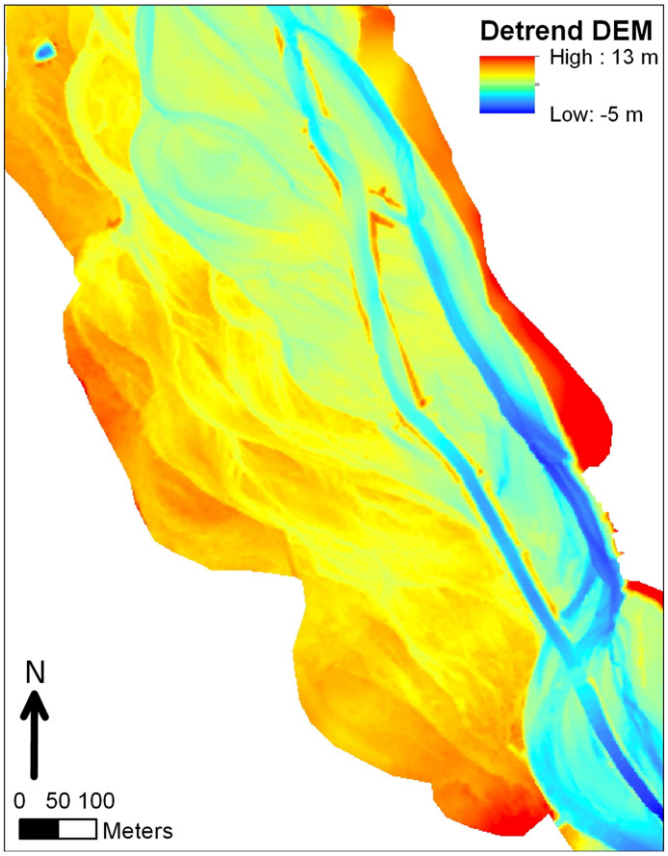


**Fig. 4.** Extract of detrended DEM on the Drôme River.

#### 3.1.2. Historical and recent aerial photographs

For the Bouinenc Torrent and the Bès River, a set of historical air photos were selected to reconstruct channel changes over a period of 62 years (1948, 1956, 1975, 1982, 1984, 1990, 1993, 2000 and 2004) (Table 3). This was completed with two recent dates (2008 and 2010) for which channel morphology was extracted from two LiDAR surveys. Each historical aerial photograph was georectified based on 2004 orthophotos. Control points were chosen only in the proximity of the river corridor, to avoid distortions due to the relief. The georectification quality was measured with the root-mean-square error (RMSE). After this pre-processing, the active channel (water and unvegetated gravel bars) and vegetated islands (pioneer and mature vegetation combined) were manually delineated by the same operator for each date.

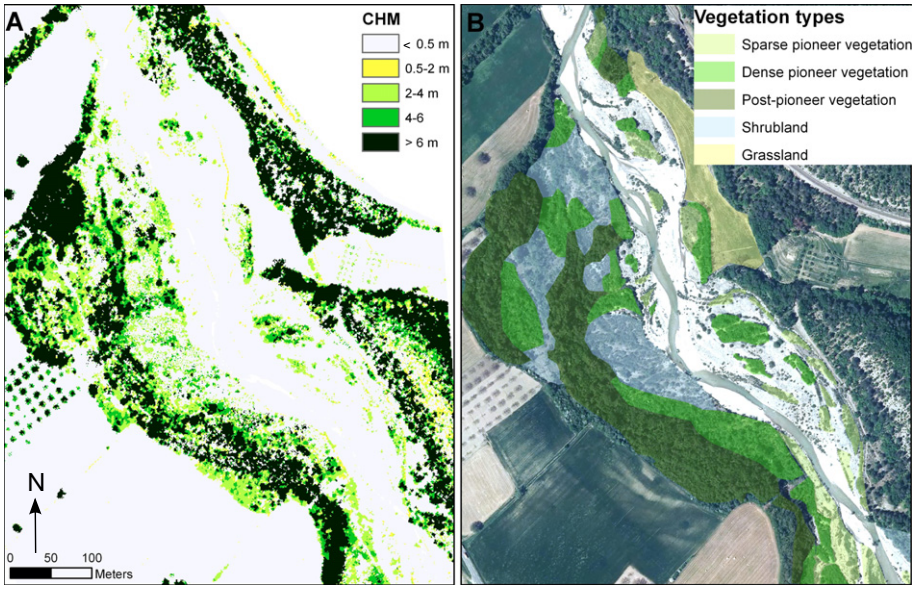


**Fig. 3.** (A) Extract of the Canopy Height Model (CHM) raster on the Drôme River; (B) example of vegetation type mapping on the 2010 orthophotos; source: IGN.

**Table 3**
Data used to reconstruct long-term channel changes of the Bès and Bouinenc study sites.

| Year | Type | Scale/Resolution | Source |
|---|---|---|---|
| 1948 | Black and white photographs | 1:30,000 | IGN |
| 1956 | Black and white photographs | 1:25,000 | IGN |
| 1975 | Black and white photographs | 1:30,000 | IGN |
| 1982 | Black and white photographs | 1:17,000 | IGN |
| 1984 | Black and white photographs | 1:30,000 | IGN |
| 1990 | Black and white photographs | 1:30,000 | IGN |
| 1993 | RGB photographs | 1:20,000 | IGN |
| 2000 | RGB photographs | 1:25,000 | IGN |
| 2004 | Orthophotos | 0.5 m | IGN |
| 2008 | Airborne LiDAR survey | 0.5 m | Irstea |
| 2010 | Airborne LiDAR survey | 0.5 m | Irstea |

For the Drôme River, active channel and vegetated islands were mapped by Toone et al. (2014) using eight series of aerial photographs (1948, 1956, 1971, 1980, 1991, 1996, 2001 and 2006) (Table 4). This work was completed with the 2010 delineation of the active channel and vegetated islands, mapped on the LiDAR-derived DSM.

### 3.2. Long-term evolution and present-day floodplain morphology

From active channel polygons, active channel widths were extracted every 10 m along the study reaches to reconstruct narrowing/widening trends over time. Between each pair of observations, the mosaic of the landscape turnover (overlay) was built according to Belletti et al. (2014) and four types of landscape changes were obtained: (1) floodplain construction (active channel becoming perennial vegetation in the floodplain), (2) island formation (active channel becoming a vegetated island), (3) floodplain erosion (perennial vegetation in the floodplain becoming an active channel) and (4) island erosion (vegetated island becoming an active channel).

The approximate age of floodplain patches was deduced from the diachronic analysis of historical air photos over the last 60 years (Dufour, 2005; Greco et al., 2007). This age corresponds to the date of definitive abandonment of a surface by the active channel, which means the area becomes vegetated by perennial vegetation. Mean relative elevations of dated floodplain patches (relative elevation above the mean active channel elevation) were measured using LiDAR data.

### 3.3. Attributes of riparian vegetation patches

Vegetation patches were photointerpreted using 2009 orthophotos and CHMs (Fig. 3B). Vegetation types were defined following Dufour's classification (2005), which is based on the pioneering studies conducted by Pautou and Girel (1986) and Marston et al. (1995) on the Ain River. Six generic types were retained: (1) sparse pioneer vegetation, (2) dense pioneer vegetation, (3) post-pioneer vegetation, (4) shrubland, (5) grassland, (6) grassland with shrub colonisation and (7) man-made vegetation (Table 5).

Some variables were extracted for each vegetation patch. Vegetation height and cover were derived from the CHM raster. Vegetation height corresponds to the mean value of pixels >0.5 m, and vegetation cover corresponds to the proportion of pixels >0.5 m. Each vegetation patch was also characterised in terms of relative elevation, area, distance to the main wetted channel and age.

We performed a multivariate statistical analysis to see how vegetation types can be distinguished according to a set of continuous variables describing local conditions in terms of vegetation and floodplain characteristics: vegetation height, vegetation cover, floodplain age, relative elevation and distance from the main channel. The median and relative interquartile ranges of these variables were used. The aim was then to maximize the ratio of between-group variance to total variance using a factorial discriminant analysis (FDA) (Lebart et al., 1995).

**Table 4**
Data used to reconstruct the long-term lateral evolution of the Drôme study site.

| Year | Type | Scale/Resolution | Source |
|---|---|---|---|
| 1948 | Black and white photographs | 1:30,000 | IGN |
| 1956 | Black and white photographs | 1:25,000 | IGN |
| 1971 | Black and white photographs | 1:25,000 | IGN |
| 1980 | Black and white photographs | 1:25,000 | IGN |
| 1991 | Colour photographs | 1:17,000 | IGN |
| 1996 | Black and white photographs | 1:25,000 | IGN |
| 2001 | Colour photographs | 1:25,000 | IGN |
| 2006 | Ortho-photographs | 0.5 m | IGN |
| 2010 | Airborne LiDAR survey | 0.5 m | Irstea |

**Table 5**
Description of vegetation units (from Dufour, 2005).

| Vegetation units | Characteristics |
|---|---|
| Sparse pioneer vegetation | Sand, gravel, and cobble deposits colonized by low willow shrubs <2–4 m high. |
| Dense pioneer vegetation | Sand, gravel, and cobble deposits with dense willows or poplars >3–4 m high |
| Post-pioneer vegetation | Mixed hardwood-softwood forest, trees >6 m high; *Populus nigra*, *Fraxinus excelsior*, *Alnus glutinosa*, *Quercus robur*, Acer spp., *Ulmus minor* |
| Shrubland | Dense, diverse, mesophytic shrubs (*Crataegus monogyna*, *Lonicera xylosteum*, *Ligustrum lantana*, *Ligustrum vulgare*, *Prunus spinosa*, *Viburnum lantana*) with some softwood trees (*Populus nigra*) |
| Grassland | Dry grassland without willows |
| Grassland with shrub colonisation | Dry grassland with some willows and spiny shrubs (*Bromus erectus* with *Salix eleagnos*, *Prunus spinosa*, *Crataegus monogyna*) |
| Man-made vegetation | Planting trees, gravel edges… |

## 4. Results

### 4.1. Floodplain history at a pluri-decadal scale

#### 4.1.1. Active channel width changes

Study reaches showed different patterns of active channel changes over the last few decades. The Drôme River showed a relatively stable active width between 1948 and 2010, with a mean value of 36 m in 1948 and 40 m in 2010 (Fig. 5 and Fig. 6A). Some periods underwent slight active channel narrowing, mainly 1956–1970, 1996–2001 and 2006–2010, whereas widening was observed for the following periods: 1948–1956 (+60 m), 1991–1996 (+49 m) and 2001–2006 (+47 m). The 1956 planform presented the highest active width and the most highly developed braided pattern. Compared to the 1956 planform, the 2010 planform showed a 33% decrease in active width and a decline of braided sections with significant reach-scale straightening in some parts (Fig. 5).

Like the Drôme, the Bès River showed a relatively stable active channel over the last 60 years, with a slight decrease in the mean active width between 1948 and 2010, 180 m and 143 m, respectively, i.e. 21% narrowing (Fig. 6B). The narrowing period was mainly between 1948 and 1975 and between 1984 and 1990. Significant active width increases were observed for the following periods: 1975–1984 (+12 m), 2000–2004 (+17 m) and 2008–2010 (+8 m) (Fig. 4B).

Active channel changes of the Bouinenc Torrent displayed a very different pattern from the two other sites. A dramatic active width decrease was observed during the period, mainly between 1948 and 1975, during which the torrent lost 73% of its active channel (Figs. 6C and 7). This resulted in a shifting pattern from braided to wandering. Since 1975, the active channel width has only very slightly increased.

#### 4.1.2. Floodplain erosion and construction linked to channel shifting

On the Drôme River, three periods were characterised by net floodplain destruction, during which active channel shifting and subsequent

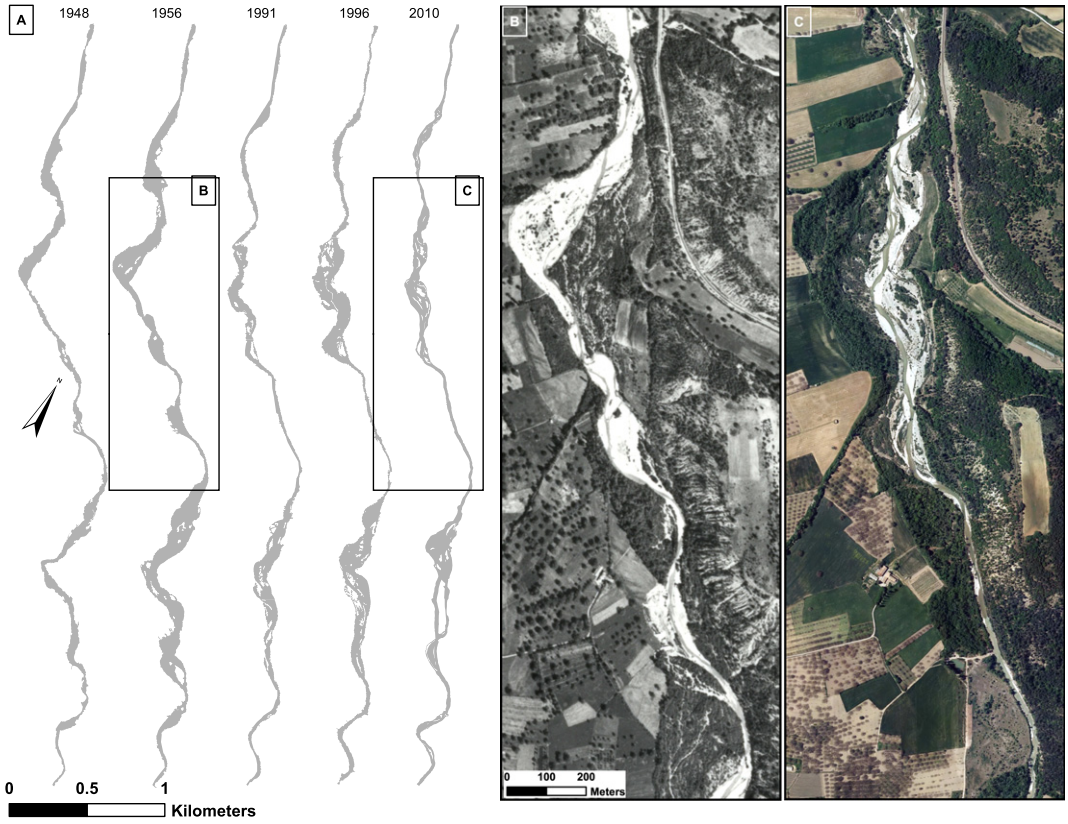


**Fig. 5.** Active channels of the Drôme River between 1948 and 2010: (A) active channel extent; (B) 1956 aerial photograph (IGN); (C) 2010 orthophotograph (IGN).

riparian vegetation rejuvenation occurred: 1948–1956, 1991–1996 and 2001–2006 (Fig. 8A). The 1971–1980 period showed a net equilibrium between floodplain erosion and construction, demonstrating considerable lateral shifting of the active channel. Other periods showed net floodplain construction with substantial vegetation encroachment. Two periods showed an increase in island formation: 1991–1996 and 2006–2010.

On the Bès River, five periods showed net floodplain construction: 1948–1956, 1956–1975, 1984–1990, 1993–2000 and 2004–2008 (Fig. 8B). This is particularly true between 1984 and 1990, where floodplain erosion represented only 12% of floodplain construction. Some periods were characterised by significant net floodplain erosion: 1975–1982, 2000–2004 and 2008–2010 (Fig. 8B). Trends affecting island surface areas did not differ from floodplain surface areas. It is nevertheless interesting to see that the absolute values of changes are equivalent for islands and floodplains, which is not the case for the Drôme where island surface areas are much lower than floodplain surface areas.

On the Bouinenc Torrent, three periods of net floodplain formation were observed (Fig. 8C). This was particularly observed between 1948 and 1975 (0.47 $m^2\ km^{-1}\ yr^{-1}$ between 1948 and 1956, and 0.18 $m^2\ km^{-1}\ yr^{-1}$ between 1956 and 1975). Periods between 1984 and 1993 show equivalent floodplain erosion and formation surface areas, demonstrating active channel shifting. The following periods were characterised by very low values of floodplain turnover, with a slight trend towards net floodplain erosion.

Floodplain turnover rates were calculated from the ratio between the mean annual floodplain erosion rate over the last 60 years and the total floodplain surface areas in 2010. The Bès River showed the highest value with a yearly floodplain turnover of 5.3%, versus 0.9% for the Drôme River and 0.6% for the Bouinenc Torrent.

*4.1.3. Relative elevation of dated floodplain surfaces*

Time variations of active channel elevation reconstructed from terrace remnants are presented in Fig. 9. On the Drôme River (Fig. 9A), the first period of incision occurred before 1948, as attested by the difference in elevation between the 1948 terrace and the floodplain surfaces already vegetated in 1948. The 1948 terrace stands 0.5 m below these surfaces. Between 1948 and 1956, the bed level was stable, and a slow incision was detected between 1956 and 1971. A rapid incision was observed between 1971 and 1996, with acceleration between 1991 and 1996 when a major flood occurred (January 1994). The 2001 remnant surfaces indicate that aggradation occurred between 1996 and 2001, but caution should be exercised for this period, since the 2001 remnant surfaces were not well preserved along the reach and are likely not representative of the bed level changes. Even if the 2001 surfaces are discarded, the 2006 surfaces indicate channel stability between 1996 and 2006, and therefore a specific signature of channel recovery during this decade, when a major flood occurred in December 2003. Finally, another rapid incision was detected between 2006 and 2010, with a rate that had not been observed before.

On the Bès River, the first period of stability or slight aggradation was observed until 1975 with a higher aggradation for the 1975 remnant surfaces. This period was followed by an abrupt incision period between 1975 and 1982, when two major floods occurred in 1977 and 1979 (Fig. 9B). A difference of 0.7 m was observed between the two surface levels. The new bed level only showed a few changes over the two decades that followed with, however, a slight incision trend. This period was interrupted by a period of aggradation between 2000 and 2004.

On the Bouinenc, the first period of incision occurred before 1948, as attested by the difference in elevation between the 1948 terrace and the floodplain surfaces already vegetated in 1948 (Fig. 9C). The 1948 terrace

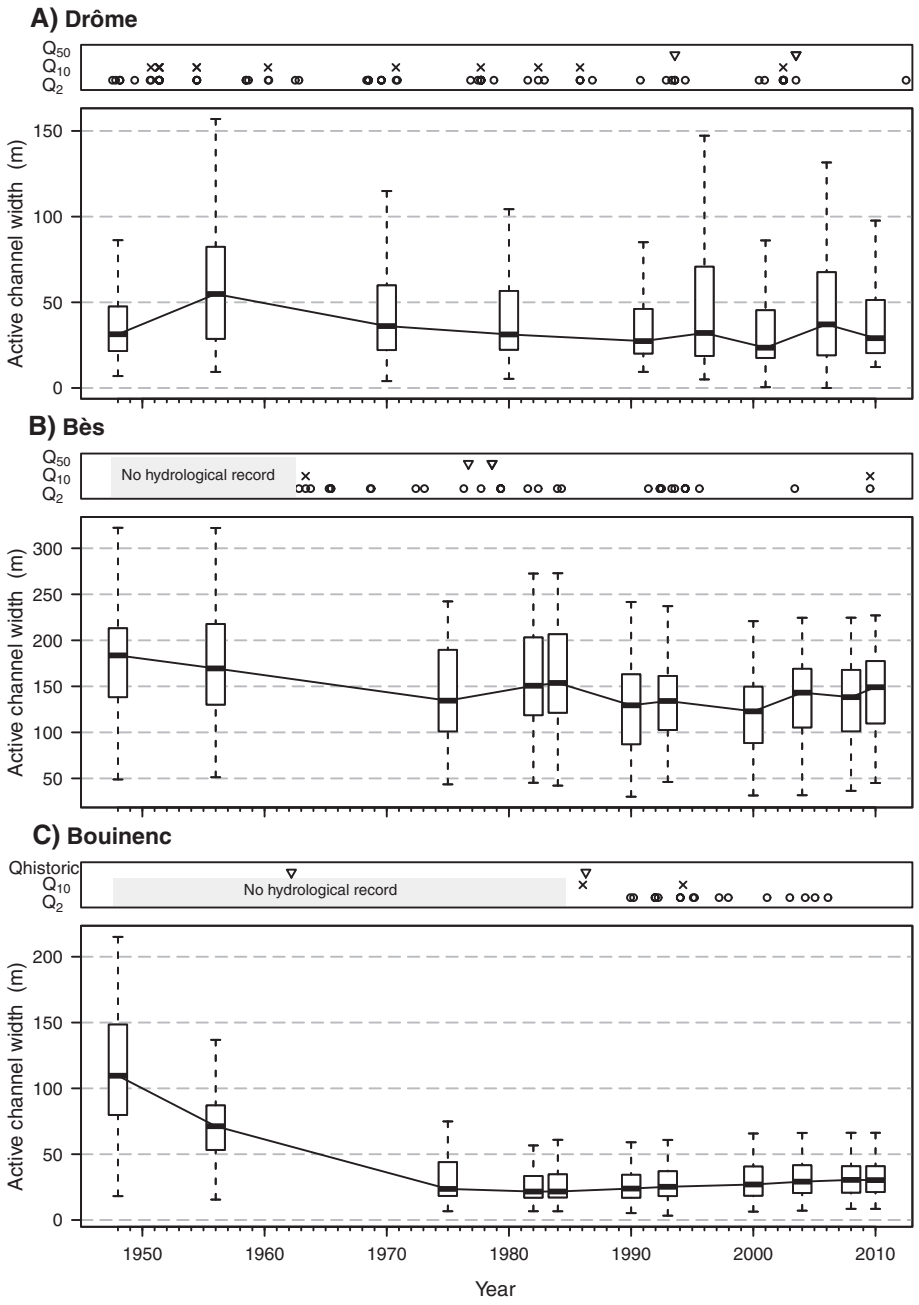


**Fig. 6.** Active channel widths between 1948 and 2010 of (A) the Drôme River; (B) the Bès River; and (C) the Bouinenc Torrent; occurrence of small (Q2 < Q < Q10), medium (Q10 > Q > Q50) and large (Q > Q50) floods are indicated at the top of the graph. The lengths of the hydrological series for each of the three sites are 1907–2014, 1963–2014 and 1983–2013, respectively. Historic floods (Qhistoric) correspond to floods recorded on BD-RTM on the Bouinenc Torrent.

stands 0.4 m below these surfaces. A second progressive incision was detected beginning in 1956 with an increased incision after 1990. This period was interrupted by two aggradation periods: the first period between 1984 and 1990 and the second between 2000 and 2008. After 1975, caution should be used because the remnant surface areas are very low.

### 4.2. Contemporary responses of riparian vegetation

#### 4.2.1. Validation of vegetation patch types from LiDAR data

Factorial discriminant analysis (FDA) by vegetation types showed that sparse pioneer, dense pioneer and post-pioneer vegetation are clearly distinguished by vegetation height, cover percentage and age (Fig. 10). These three units showed typical changes in vegetation characteristics following the classic ecological succession. Sparse pioneer vegetation patches had the lowest heights and cover percentages. Dense pioneer vegetation patches were slightly taller but much denser than sparse-pioneer vegetation patches. Post-pioneer vegetation patches presented the highest heights and cover percentages. Shrubland vegetation had intermediate height and cover percentage and differed from the other types in its higher relative elevation and the high variability in vegetation height. This may be related to different local conditions, possibly drier, limiting recruitment and growth to a dense riparian unit.

#### 4.2.2. Inter-site comparison of vegetation patch types

The vegetation mosaic between the three reaches was fairly contrasted, as confirmed by the chi-square test (Table 6). The Bès River is characterised by a high proportion of sparse pioneer vegetation, the Bouinenc River by a high proportion of shrubland. The Drôme River

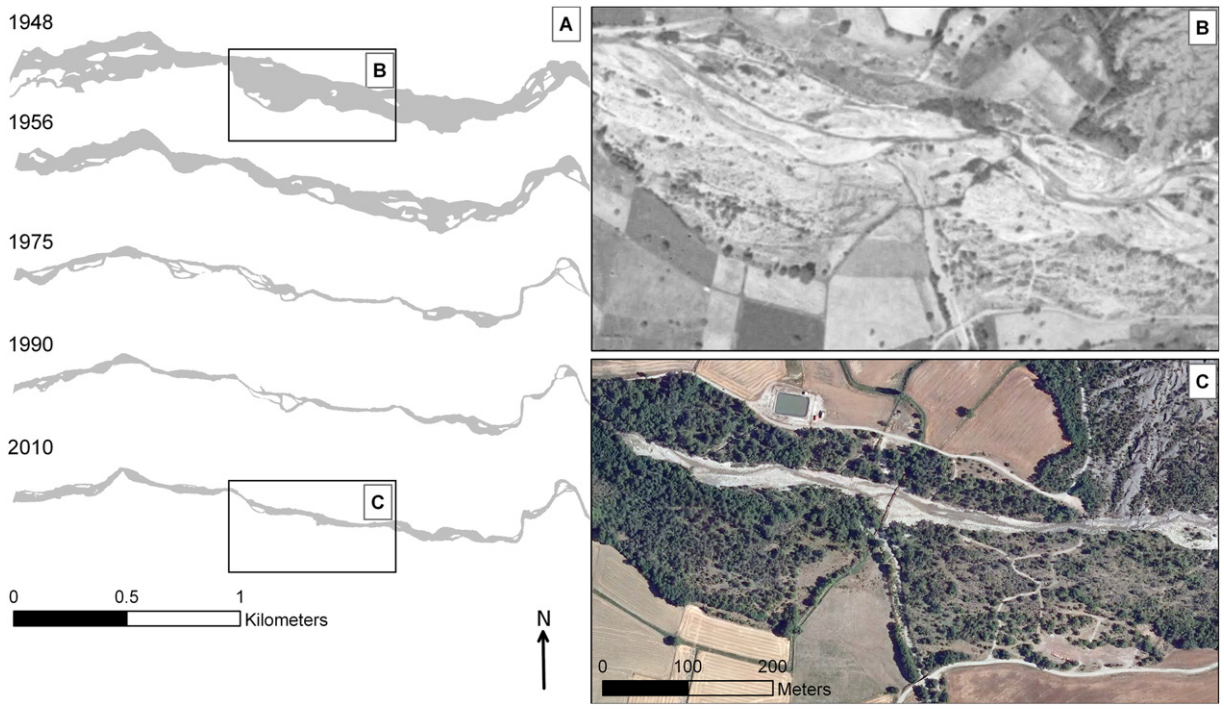


**Fig. 7.** Active channels of the Bouinenc Torrent between 1948 and 2010: (A) active channel extent; (B) 1948 aerial photograph (IGN); (C) 2009 orthophotograph (IGN). Extent of vegetated floodplain observed on 2009 photograph corresponds to the extent of active channel in1948.

is characterised by a more equi-distribution of vegetation types (Fig. 11).

*4.2.3. Type and characteristics of vegetation patches over time*

On the Drôme, shrublands established at different periods (Fig. 12A). Post-pioneer and dense-pioneer patches also occurred over the whole period. Sparse pioneer vegetation was observed between 1980 and 1991. Some of these patches did not evolve to post-pioneer vegetation, which can be surprising because the successional trend is not as clear here. Younger surfaces were dominated by sparse vegetation.

On the Bès, the succession organisation is much clearer, with sparse vegetation dominant on the younger surfaces and then replaced by dense-pioneer and post-pioneer vegetation (Fig. 12B). Post-pioneer vegetation was then dominant before the 1980s with a small patch of shrubland established during the 1956–1975 period. Sparse and dense-pioneer patches also occurred in the 1990s.

On the Bouinenc Torrent, vegetation established prior to 1975 was predominantly both mature forest and shrubland (Fig. 12C). In the recent period, shrubland almost disappeared, the mature vegetation decreased in frequency where the dense-pioneer and the sparse-pioneer vegetation became dominant. The age gradient was again well established. A surprising peak of dense pioneer patches was observed between 1990 and 1993 and also to a lesser extent for sparse pioneer vegetation.

Consequently, shrubland units and mature riparian units are approximately the same age but regarding the relative elevation, it can be observed that shrubland units had clearly higher relative elevation than post-pioneer vegetation on the Drôme and the Bès (Fig. 13). The elevation difference was lower for the Bouinenc Torrent.

## 5. Discussion

In this study, we fused information delivered by sequenced historical aerial photos and LiDAR data to better understand river-floodplain dynamics, most particularly the relation between vertical and lateral channel changes, vegetation responses and flood occurrence. Fig. 14 summarises changes over time in terms of lateral and altimetric channel changes as well as vegetation units for the three different rivers.

*5.1. River-floodplain dynamics*

Fusion of information delivered by historical aerial photos and LiDAR data revealed an early period of channel incision starting before 1948 for the Drôme River and the Bouinenc Torrent. Previous field investigations along tributaries to the Drôme River have already shown the existence of a terrace level occupied by trees established in the 1920s, which was attributed to the cumulative effect of the climate change following the end of the Little Ice Age and torrent control works of the 1860–1914 period (Liébault and Piégay, 2002; Liébault et al., 2008). This phase has also been identified for Italian rivers and referred to a first phase of channel adjustment, characterised by channel narrowing and incision (Surian, 2009; Ziliani and Surian, 2012). These new results demonstrate that this incision phase is relatively large, which was not shown in previous studies, due to the absence of topographic data for this period.

During the second half of the 20th century, bed-level evolution and lateral morphological changes show contrasting responses between sites. On the Drôme River, channel incision starts in the 1970s and is therefore not associated with long-term narrowing, whereas these two adjustments are often associated in channel evolution models during this period (e.g. Bollati et al., 2014). This period corresponds to the onset of an active period of gravel mining in this valley (Stella et al., 2013), which stopped in the early 1990s with the prohibition of gravel mining in active channels (passed by the Ministry of the Environment in 1994). An acceleration of channel incision is observed between 1991 and 1996, with a major flood occurring in January 1994. Another major flood occurred in 2003 but did not induce a significant incision. This contrasting response can be linked with the cessation of gravel mining, which has likely contributed to channel recovery by preventing any further sediment deficit. The onset of another accelerated incision from 2006 onward is more difficult to explain, but the real existence of this late incision phase must be questioned since the 2006 remnant surfaces are highly localised and may not be representative of the

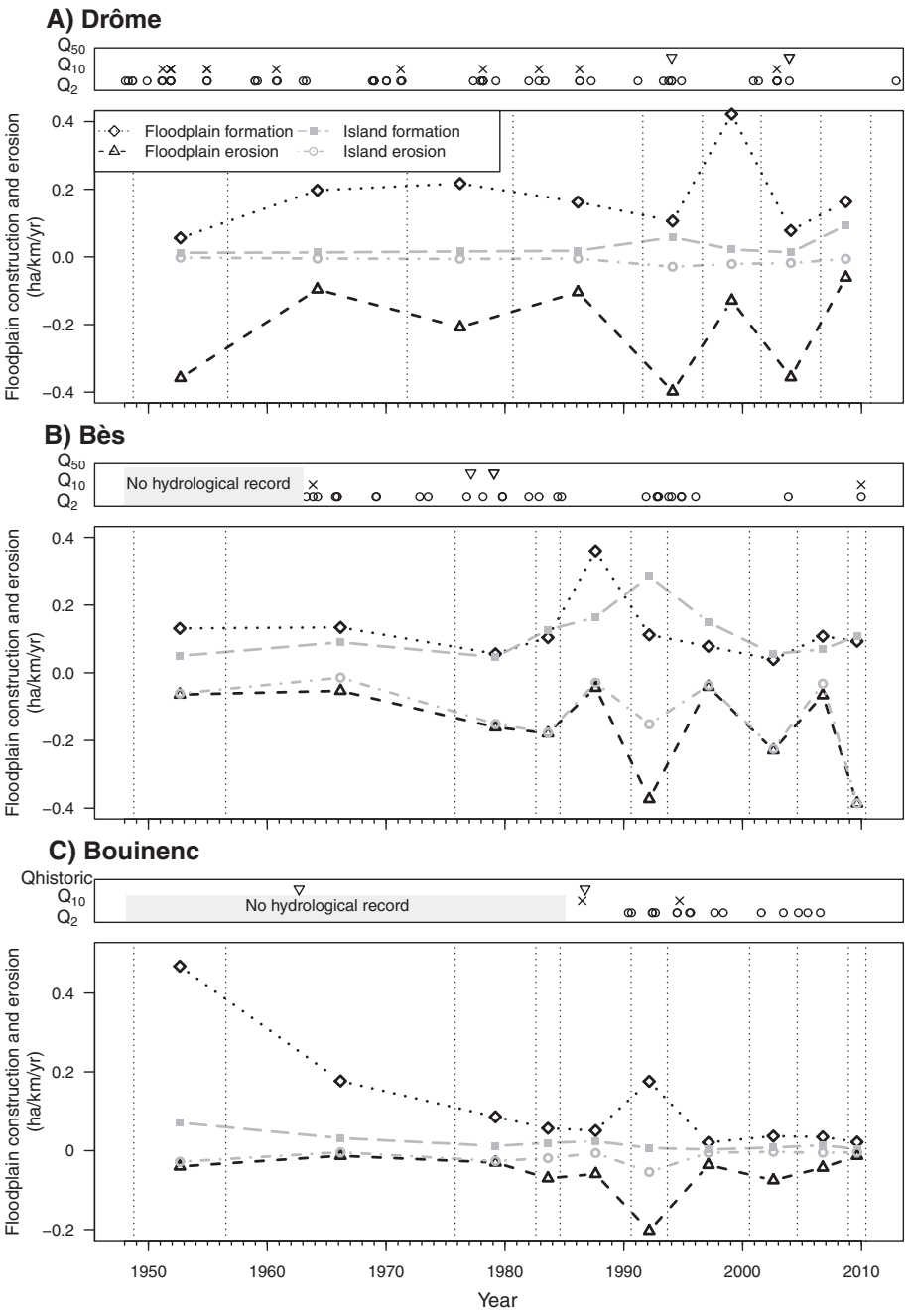


**Fig. 8.** Floodplain construction and erosion for each study reach over time: (A) Drôme River; (B) Bès River; (C) Bouinenc Torrent. Occurrence of small (Q2 < Q < Q10), medium (Q10 > Q > Q50) and large (Q > Q50) floods are indicated at the top of the graph. Historic floods (Qhistoric) correspond to floods recorded on BD-RTM on the Bouinenc Torrent. Dotted vertical lines correspond to the date of aerial photographs.

whole reach. This has not been confirmed by recent long profile surveys in this reach, in which no incision was detected.

On the Bès, no long-term pattern of widening or narrowing was observed and slight incision is detected after the occurrence of two major floods in 1977 and 1979. An aggradation was observed, however, between 2000 and 2004. This aggradation is probably related to a flood occurring in November 2000. In fact, hydrological data on the Bès River have not recorded significant floods at the Pérouré gauging station during this period. However, BD-RTM recorded a flood in November 2000 that caused a great deal of damage upstream from the study reach such as bed scouring inducing the destruction of a bridge and bank erosion.

On the Drôme and Bès Rivers, lateral fluctuations are significantly associated with large and medium floods, although this link is complex. On the Drôme, medium floods had greater effects in the 1950s than today. This could be the consequence of a decreasing sediment supply from the Béoux, where active channel narrowing is observed (Liébault, 2003).

This is not the case of the Bès, where strong responses to medium floods are still observed today, because of the high sediment supply from the catchment. First, this study confirmed the impact of the flood pulse (with a return period higher than 2 years) and in particular a 10-year flood return period on braided river morphology, which had already been shown by previous authors (Bertoldi et al., 2010; Belletti et al., 2014). Secondly, it seems that channel shifting is exacerbated in active bedload transport conditions and slows down when sediment supply and bar dynamics are reduced, as shown by Constantine et al. (2010); Alber (2012); Toone et al. (2014) and Belletti et al. (2014).

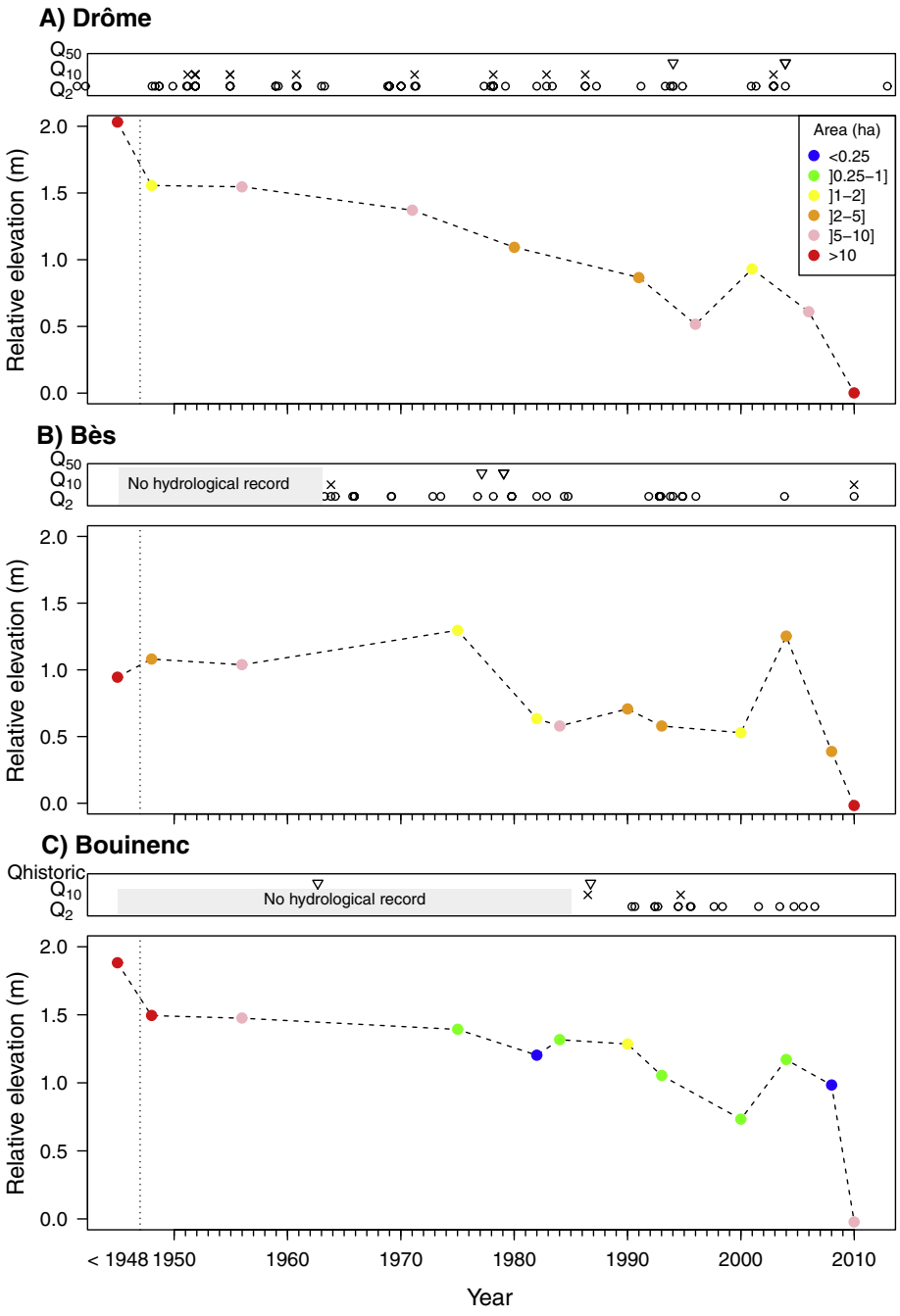


**Fig. 9.** Relative elevation of remnant surface over time of (A) the Drôme River; (B) the Bès River; and (C) the Bouinenc Torrent; Standard errors are lower than the size of the symbol. Colours indicate the area interval of the remnant surface. Occurrence of small (Q2 < Q < Q10), medium (Q10 > Q > Q50) and large (Q > Q50) floods are indicated at the top of the graph. Historic floods (Qhistoric) correspond to floods recorded on BD-RTM on the Bouinenc Torrent.

On the Bouinenc torrent, long-term active channel narrowing was observed between 1948 and 1975, in accordance with the model description for the small torrents in the Drôme, Eygues and Roubion catchments (Liébault and Piégay, 2002; Liébault et al., 2005). This can be interpreted as an effect of a sediment supply decrease due to spontaneous reforestation after the Second World War, already demonstrated in the Southern Prealps and associated with rural depopulation (Taillefumier and Piégay, 2003). This is confirmed by the slow progressive channel incision observed since the 1950s. Medium floods, which occurred in 1962, 1986 and 1994, had no significant effect on the active channel width. The second incision phase, which started in the 1990s, is more difficult to explain. One possibility is that it corresponds to the recovery of a possible aggradation following the large 1986 and 1994 floods (attested by the comparison of 1984 and 1990 remnant surfaces). Similar to the most recent period on the Drôme reach, recent floods (1962, 1986 and 1993) had no effect on the channel because there was no sediment available to promote flow divergence in the channel and maximize shear stress on banks and widen the active channel to the1948 level.

Finally, it seems that relative elevation between the channel and the different floodplain levels is not only linked to channel incision, but also to gravel progradation on the lowest floodplain levels that were still very connected to the overflows during high floods. This is particularly true for some of the lower floodplain levels observed on the Drôme

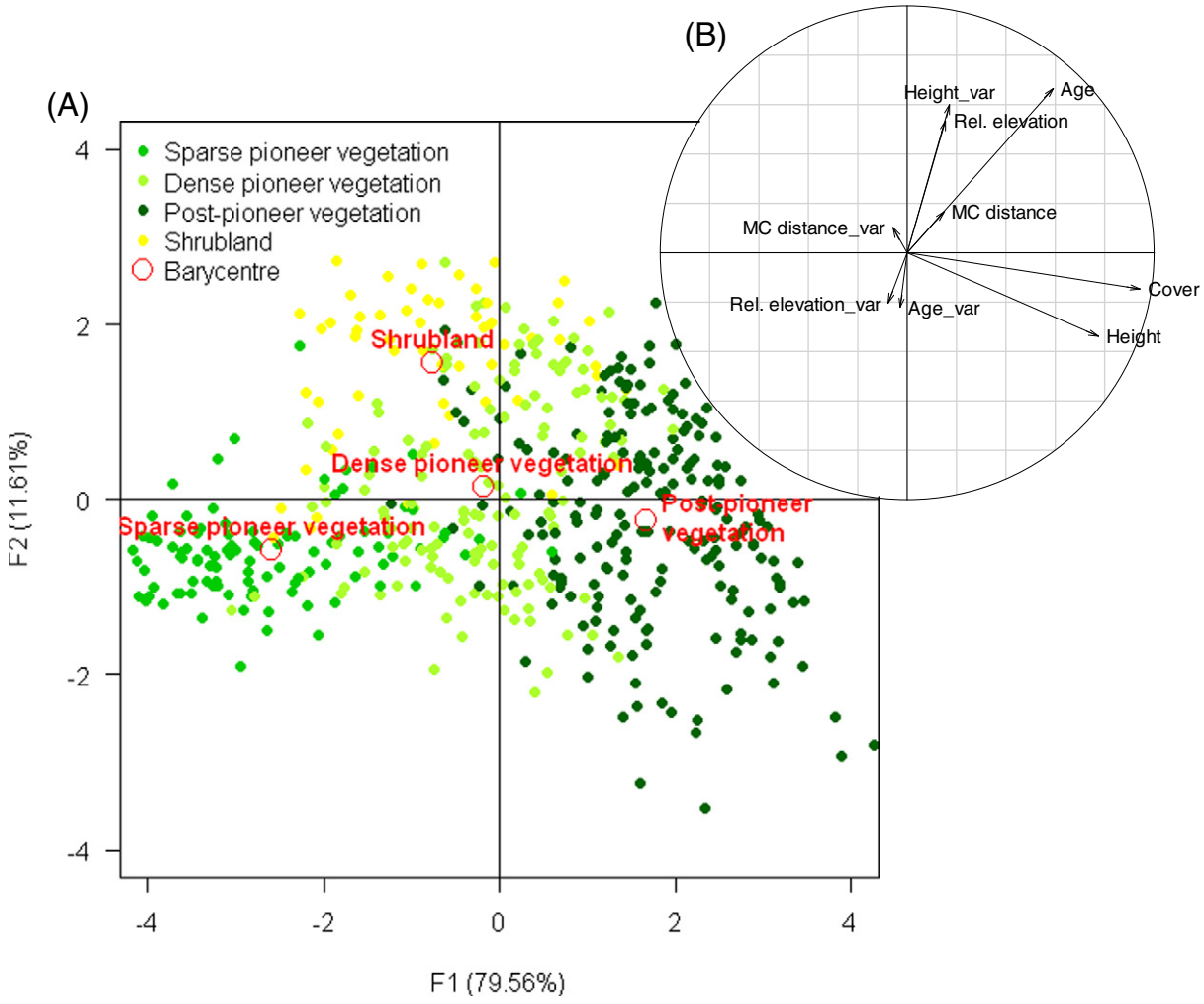


**Fig. 10.** Results of the FDA discriminated by vegetation type: (A) the F1 × F2 factor map displaying vegetation patches in vegetation type; (B) the correlation circle of variables corresponding to statistical characteristics of vegetation patches (median and relative interquartile range: "_var"). Height: vegetation height, Age: floodplain age; Rel. elevation: relative elevation; MC distance: distance from main channel median; Cover: vegetated cover percentage.

prior to the 2003 flood or on the Bès prior to the 1977 and 1979 Q50 floods.

### 5.2. Impacts of long-term changes on the contemporary vegetation mosaic

Long-term geomorphic changes play a significant role in explaining vegetation mosaics. Long-term narrowing of the Bouinenc Torrent until 1975 resulted in a well-developed vegetated floodplain for the most part composed of mature units (shrubland and post-pioneer units), which have undergone very little turnover. Still active, the Bès River shows a lower vegetated floodplain but a much better equi-distribution of different vegetation units related mainly to a higher turnover rate. This is also true for the Drôme, where all vegetation units are equi-represented. However, the presence of denser pioneer vegetation than along the Bès River shows a river that is less active than the Bès, as attested by the turnover rate, and therefore has much more homogeneous vegetation mosaics. Evidently vegetation responds fairly quickly and significantly to a reduction in river dynamism.

**Table 6**
Result of the chi-square test.

| Residuals (adjusted) | Drôme | Bès | Bouinenc |
|---|---|---|---|
| Sparse pioneer vegetation | **106.4** | **166.2** | **−278.4** |
| Dense pioneer vegetation | **198.4** | **−136.0** | **−76.3** |
| Post-pioneer vegetation | **−176.0** | **144.7** | **43.7** |
| Shrubland | **−53.8** | **−190.8** | **246.8** |

*The values in bold are significant at alpha level = 0.05*

In term of riparian vegetation succession, these results show that in a context of braided rivers with high rates of morphological change (e.g., on the Bès River), the different stages of the ecological succession cycles described among others by Marston et al. (1995) or Corenblit et al. (2011) are well established. In this context, bedload transport and associated channel shifting are really the drivers of vegetation mosaics (Florsheim et al., 2008), and flood induced total vegetation rejuvenation in some parts of the river corridor while in other areas, flood disturbances are low or null allowing floodplain evolution to more mature stages. It is shown on the Bouinenc that reduction in bedload transport results in vegetation encroachment; here the mature stages are dominant with the stabilisation of islands, banks and floodplains and the disconnection of vegetation from the direct influences of hydrogeomorphic disturbances.

This comparative approach shows how significant is the bedload transport driver and really questions the role of ecosystem engineers and the mutual interactions between plants and river processes as formalized by Corenblit et al. (2011). It seems demonstrating that such relations are not so mutual and that physics is the main control of vegetation which can establish or not according to channel activity. It should exist a domain for mutual interactions but it is a changing point which is temporally or spatially infrequent, a stage among many. Following Belletti et al. (2015) who explored a larger regional

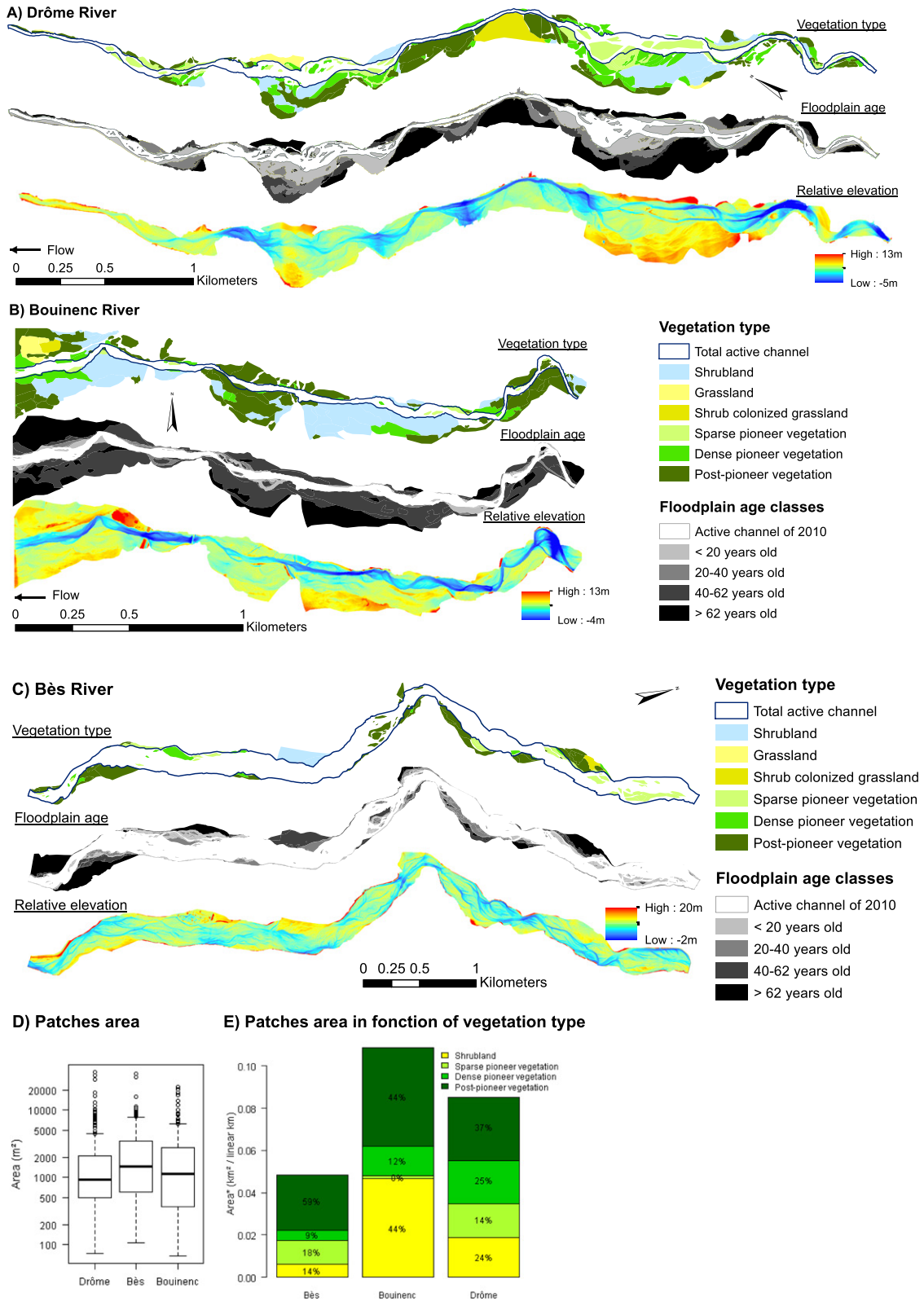


**Fig. 11.** Map of vegetation units, floodplain age classes and relative elevation for the Drôme River (A); the Bouinenc Torrent (B); and the Bès River (C); (D) boxplot of patch area for each study reach; (E) corresponding area of each type of vegetation (except grassland). Percent in each box corresponds to the percent of each type for each study reach.

scale, vegetation controls can differ from one region to another, and then the mutual interactions between hydromorphological and ecological assemblages, potentially depending on climate conditions and connectivity, can also be more frequent in given regions according to their position on the disturbance and sediment supply gradient shown by Piégay et al. (2009) and Corenblit et al. (2011). Findings also show that mutual interactions strongly depend on the intensity of channel changes. When incision occurs rapidly, floodplain is fairly high, then

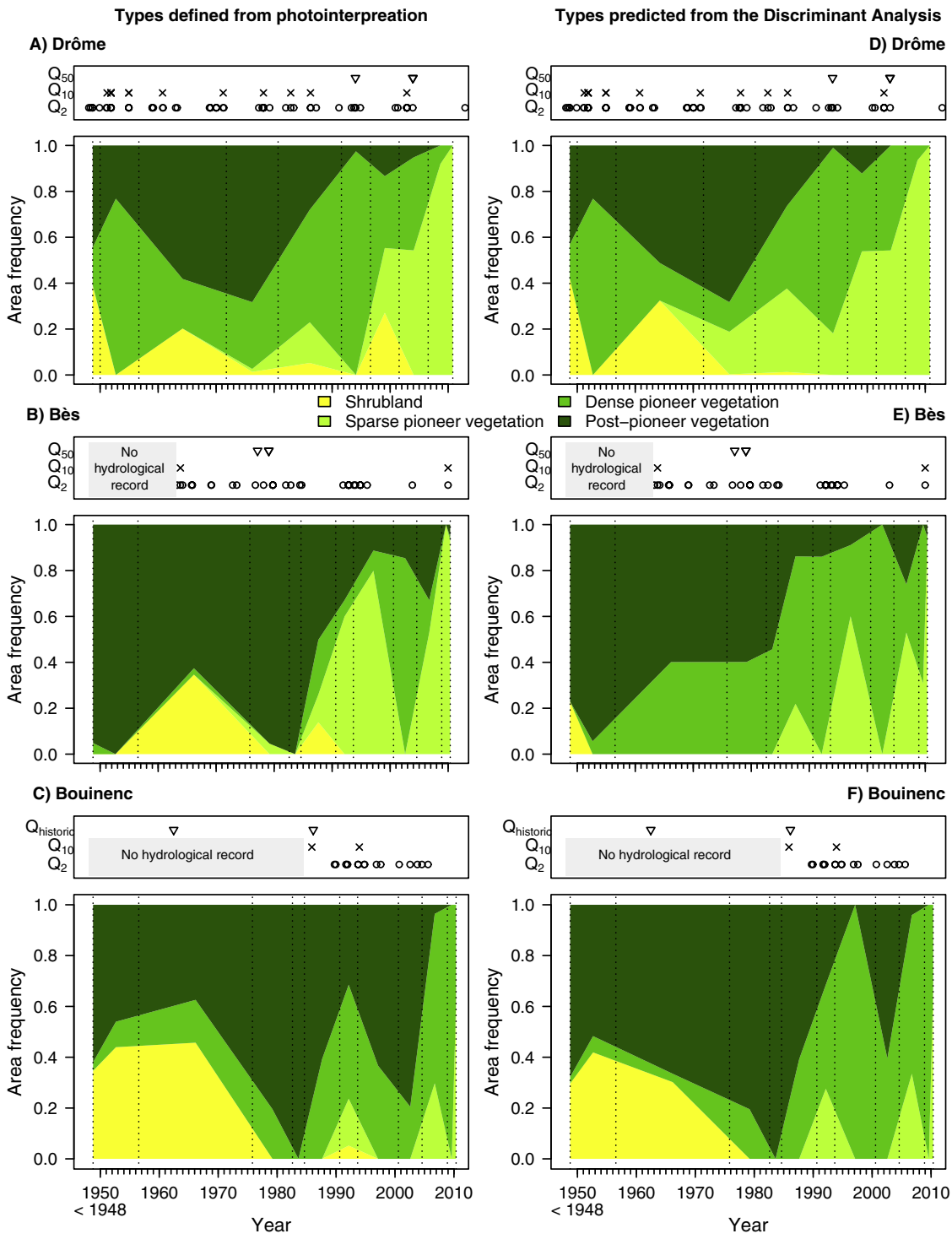


**Fig. 12.** Frequency of vegetation types per period of floodplain construction following photointerpretation protocol proposed by Dufour (2005) for (A) the Drôme River; (B) the Bès River; (C) the Bouinenc River and frequency of vegetation types per period of floodplain construction predicted from the FDA for (D) the Drôme River; (E) the Bès River; (F) the Bouinenc River. Occurrence of small (Q2 < Q < Q10), medium (Q10 > Q > Q50) and large (Q > Q50) floods are indicated on the top of the graph. Historic floods (Qhistoric) correspond to floods recorded on BD-RTM on the Bouinenc Torrent; Dotted vertical lines correspond to the date of aerial photographs.

dry and infrequently flooded and filled by fine sediment so that vegetation encroaches very slowly, reducing its potential effect on sediment trapping and bank resistance.

Both the Bès and the Drôme Rivers show greater habitat diversity than the Bouinenc River, but the Drôme River, less active than the Bès River, shows a higher vegetated floodplain than the Bès River. Consequently, as shown on the Magra River, the progressive evolution from a bar-braided pattern to a single-thread system generates a decrease in channel and bar habitats as well as the expansion of woodland units (Dufour et al., 2015). In terms of landscape diversity, Dufour et al. (2015) showed that higher active rivers present lower landscape diversity due the domination of bar units with fewer vegetation units.

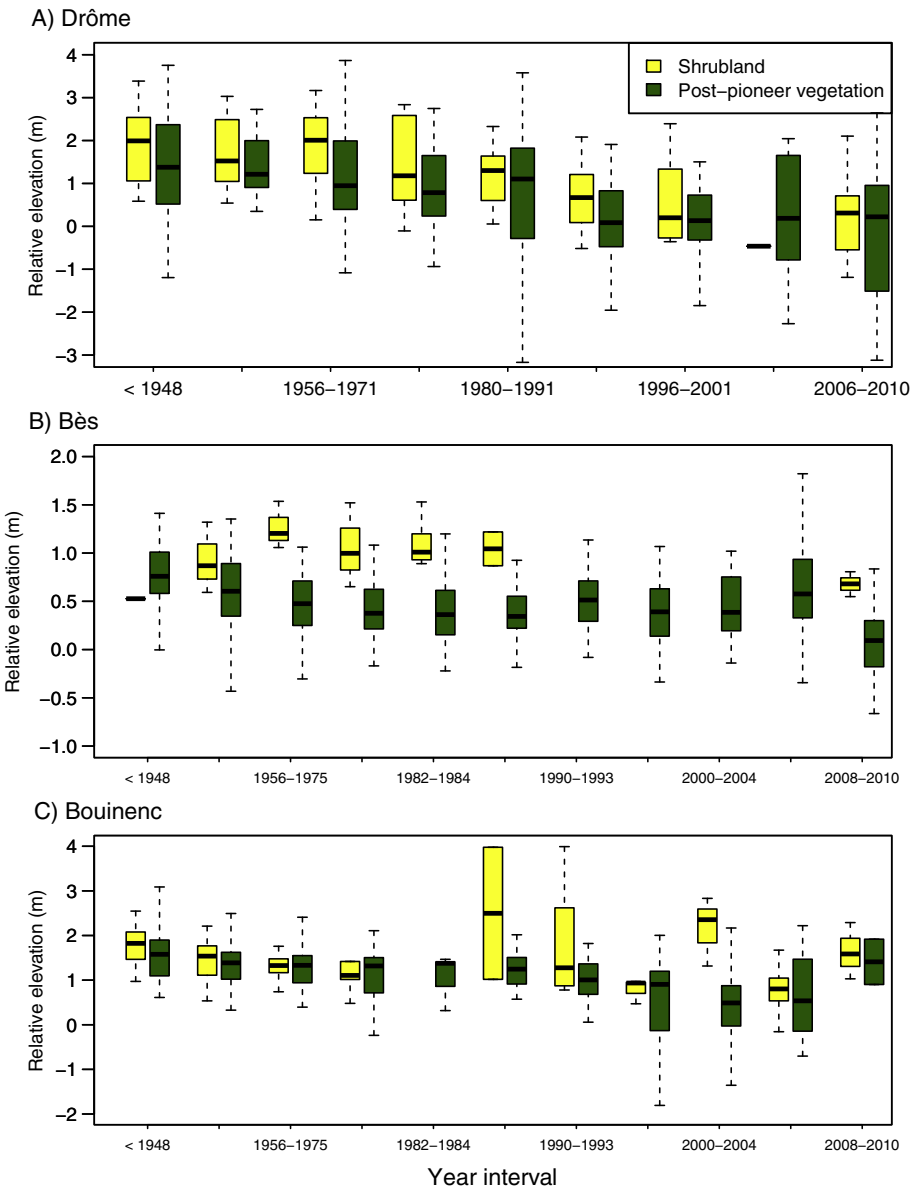


**Fig. 13.** Relative elevation of shrubland and post-pioneer vegetation units per period of floodplain construction of (A) the Drôme River; (B) the Bès River; (C) the Bouinenc River.

However, as confirmed in this present study, they showed that these rivers exhibit advantageous ecological habitats such as pioneer units, maintaining a diversity of ages and species within riparian forests.

On the three rivers, the shrubland area concerned floodplain surfaces preceding periods of high bed-level incision. Therefore, shrubland patches seem to be a good indicator of the incision period. Vegetation development is strongly affected by high floodplain surface elevation compared to the water table level (Stella et al., 2013; Singer et al., 2014). Therefore, incision impacts vegetation by disconnecting it from the water level and preventing vegetation recruitment and seed colonisation by hydrochory. For example, on the Drôme Stella et al. (2013) showed that the riparian forest decline stems from bed incision associated with drought years.

Shrubland units have approximately the same age of mature riparian units but different physiognomic characteristics. LiDAR data confirmed that these units are more frequent on fairly higher elevation units than post-pioneer units, giving greater value to the interpretation that this difference in physiognomy is related to drier conditions, explaining lower tree density and height. These units clearly describe the long-term floodplain changes and can be a proxy of terrace development in the sense they are less and less effectively connected to the present functioning of the river channel.

### *5.3. LiDAR advantages for long-term river adjustment and vegetation responses*

In this study, fusion of information delivered by sequenced historical aerial photos and LiDAR data make it possible to obtain a detailed temporal pattern of incision at a decadal scale and to closely compare it to the pattern of lateral changes. This methodology is not dependent on archived topographic data, which can be unavailable or acquired sparsely in space and time for studying the timing of incision (Bollati et al., 2014; Arnaud et al., 2015).

Due to temporal resolution of historic aerial imagery, with a 10-year interval, this method does not allow the short-term study of scour/fill and a detailed analysis of vegetation encroachment. Consequently, short-term scour/fill are not included in turnover rate computation. However, numerous authors show the importance of large and medium flood for braided river planform (Bertoldi et al., 2010; Belletti et al., 2014), so it is important that photos are relatively close to these floods

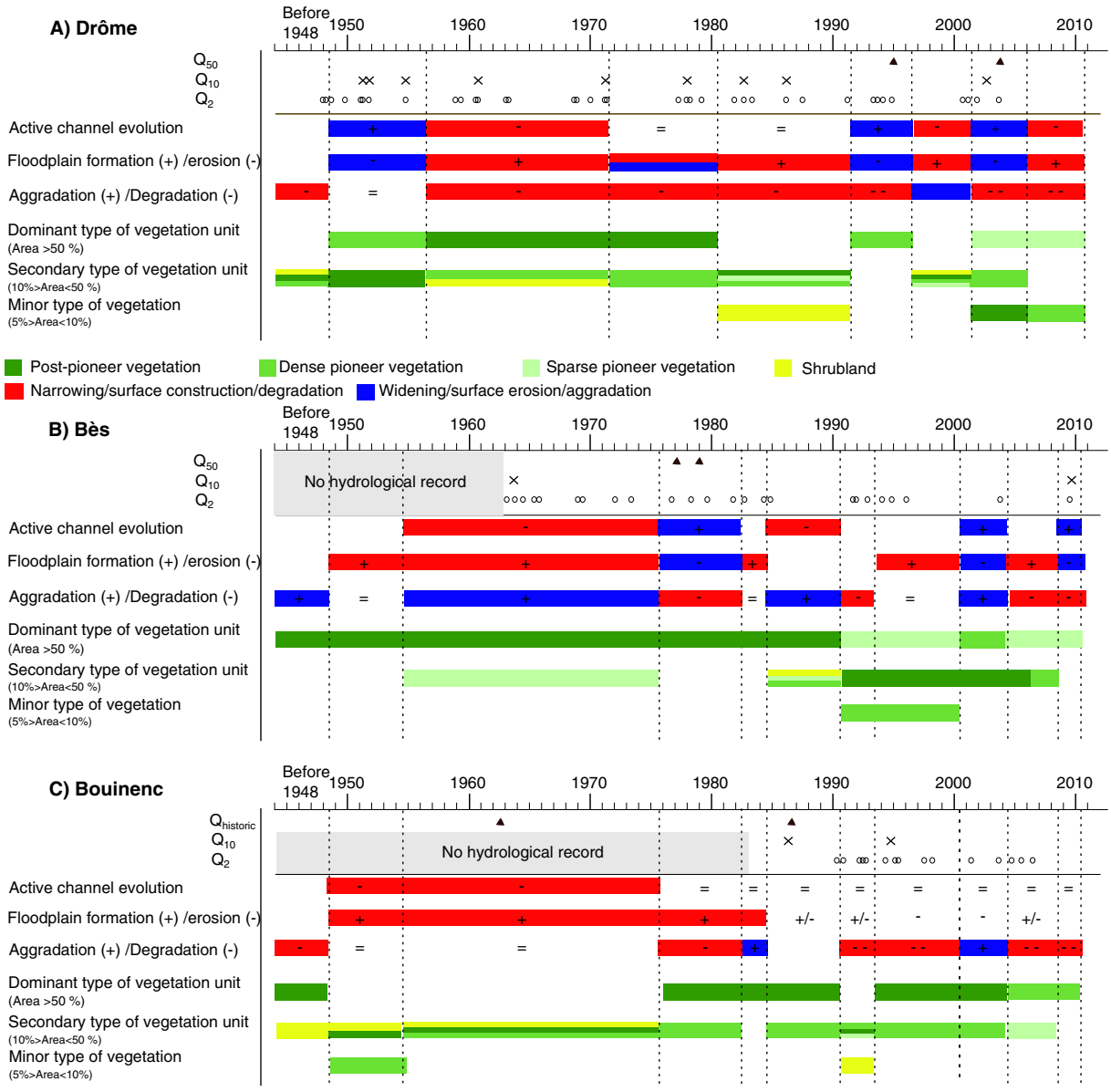


**Fig. 14.** Summary diagram of lateral and vertical evolution of active channel and vegetation characteristics over time for (A) the Drôme River; (B) the Bès River; (C) the Bouinenc River. Occurrence of small (Q2 < Q < Q10), medium (Q10 > Q > Q50) and large (Q > Q50) floods are indicated at the top of the graphs. Historic floods (Qhistoric) correspond to floods recorded on BD-RTM on the Bouinenc Torrent.

to record their effects, and 10-year intervals are then accurate to catch the main lateral movements in such rivers. In addition, this study did not investigate the mechanism of vegetation recruitment and the role of vegetation in fluvial landform dynamics, which has been highlighted by other authors (Corenblit et al., 2007; Gurnell, 2014), because the temporal scope is not accurate given that it combined biogeomorphological processes and longer-term channel changes. In fact, it would be interesting to use LiDAR data and aerial photos recorded more regularly to study this interaction in greater detail as explored by new contributions (e.g. Hortobágyi et al., 2015; Räpple et al., in press), but this is still an ongoing process requiring the much higher temporal resolution data often provided by Unmanned Aerial Vehicle (UAV) platforms.

Secondly, this methodology also makes it possible to generalize information at the scale of the entire floodplain and not to be limited to a few cross sections or local points levelled in the field for topographic data and to local sampling for vegetation so that we can better assess the respective effects of different phases of changes in space.

Finally, the combination of vegetation characteristics derived from LiDAR data and age determination from sequenced aerial photos gives good results in terms of vegetation unit classification, as shown by the confusion matrix (Table 7). The three classes (sparse, dense pioneer and post-pioneer vegetation) show typical changes in vegetation characteristics following the classical ecological succession in terms of

**Table 7**
FDA confusion matrix discriminated by vegetation type.

| From\to | Sparse pioneer | Dense pioneer | Post-pioneer | Shrubland | Total | % correct |
|---|---|---|---|---|---|---|
| Sparse pioneer | 84 | 17 | 0 | 2 | 103 | 82% |
| Dense pioneer | 14 | 106 | 9 | 14 | 143 | 74% |
| Post-pioneer | 1 | 26 | 168 | 7 | 202 | 83% |
| Shrubland | 6 | 10 | 5 | 36 | 57 | 63% |
| Total | 105 | 159 | 182 | 59 | 505 | 78% |

height and density. However, several misclassifications in the vegetation succession model are observed. This is particularly true on the Drôme River, where dense pioneer vegetation patches were observed for all ages. This was also observed on the Bouinenc River. Possible explanations may be related to human interventions on vegetation, disturbing vegetation succession, which may explain a contradiction between the physical setting (relative elevation, unit age) and vegetation characteristics (height and density) or photointerpretation misclassifications. Twenty-two per cent of the units are misclassified according to the FDA confusion matrix (Table 7). Notably, shrublands are only well classified 63% of the time and can be misclassified 18% of the time as dense pioneer vegetation, and also significantly misclassified with sparse pioneer and post-pioneer units. Fig. 12C, D and E redraws the frequency of vegetation types per period of floodplain construction for which the vegetation types are predicted from the FDA. In this figure, many of the misclassifications in succession models are no longer observed. Classification of vegetation patches from combined LiDAR information (tree density and height, relative surface elevation) and sequential aerial photo information (surface age) should allow more objective vegetation classification: the present study provides the discriminant functions for this task.

## 6. Conclusion

This research illustrates that the timing of the channel incision can be highlighted from a combination of a single LiDAR survey and historical aerial photos at the kilometre scale, two sources of data that are increasingly available. This study underlines two major periods of incision, one starting before 1948 and a second in the second half of the 20th century. Flood intensity controls smooth or abrupt channel incision, with high incision for $Q_{50}$ floods in the context of a sediment supply deficit. Large and medium floods induce channel widening with decreasing impacts in limited sediment supply conditions. Vegetation patch characteristics, such as vegetation height and density, can be obtained with this combined method and related to the geomorphic pattern and changes.

Compared to previous studies, this fusion method provides a good understanding of channel incision when archived topographic data are not valuable or sparsely distributed in space and time. Photointerpretation classes of physiognomic vegetation units are fully validated by LiDAR data and age patches established from overlays of the different channel positions observed on the historical aerial series using FDA. This approach also provides insights into identifying misclassifications and their interpretation and opens promising perspectives to use these data to automatically map physiognomic units and to explore and interpret landscape ecological patterns.

## Acknowledgements

This work was funded by the ANR Risknat Gestrans project (ANR-09-RISK-004/GESTRANS). LiDAR surveys on the Bès River were funded by CNRS-INSU (EC2CO-CYTRIX program). The study also benefited from the ORE Draix-Bléone and ZABR research networks. SMAVD (Syndicat Mixte de la Rivière Drôme) is acknowledged for providing airborne LiDAR coverage of the Drôme. We kindly thank Linda Northrup for improving English and the anonymous reviewers for their advice.

## References

Alber, A., 2012. Etude multi-scalaire de la dynamique latérale des tronçons fluviaux PhD Thesis Université Lumière Lyon 2, Lyon (262 pp).

Arnaud, F., Piégay, H., Schmitt, L., Rollet, A.J., Ferrier, V., Béal, D., 2015. Historical geomorphic analysis (1932–2011) of a by-passed river reach in process-based restoration perspectives: the Old Rhine downstream of the Kembs diversion dam (France, Germany). Geomorphology 236, 163–177.

Belletti, B., Dufour, S., Piégay, H., 2014. Regional assessment of the multi-decadal changes in braided riverscapes following large floods (example of 12 reaches in South East of France). Adv. Geosci 37, 57–71.

Belletti, B., Dufour, S., Piégay, H., 2015. What is the relative effect of space and time to explain the braided river width and island patterns at a regional scale? River Res. Appl. 31, 1–15.

Bertoldi, W., Zanoni, L., Tubino, M., 2010. Assessment of morphological changes induced by flow and flood pulses in a gravel bed braided river: the Tagliamento River (Italy). Geomorphology 114, 348–360.

Bertoldi, W., Gurnell, A.M., Drake, N.A., 2011. The topographic signature of vegetation development along a braided river: results of a combined analysis of airborne lidar, color air photographs, and ground measurements. Water Resour. Res. 47, W06525.

Bertoldi, W., Gurnell, A.M., Welber, M., 2013. Wood recruitment and retention: the fate of eroded trees on a braided river explored using a combination of field and remotely-sensed data sources. Geomorphology 180, 146–155.

Bollati, I.M., Pellegrini, L., Rinaldi, M., Duci, G., Pelfini, M., 2014. Reach-scale morphological adjustments and stages of channel evolution: the case of the Trebbia River (northern Italy). Geomorphology 221, 176–186.

Clerici, A., Perego, S., Chelli, A., Tellini, C., 2015. Morphological changes of the floodplain reach of the Taro River (Northern Italy) in the last two centuries. J. Hydrol. 527, 1106–1122.

Constantine, J.A., Dunne, T., Piégay, H., Kondolf, G.M., 2010. Controls on the alluviation of oxbow lakes by bed-material load along the Sacramento River, California. Sedimentology 57, 389–407.

Corenblit, D., Tabacchi, E., Steiger, J., Gurnell, A.M., 2007. Reciprocal interactions and adjustments between fluvial landforms and vegetation dynamics in river corridors: a review of complementary approaches. Earth Sci. Rev. 84, 56–86.

Corenblit, D., Baas, A.C.W., Bornette, G., Darrozes, J., Delmotte, S., Francis, R.A., Gurnell, A.M., Julien, F., Naiman, R.J., Steiger, J., 2011. Feedbacks between geomorphology and biota controlling Earth surface processes and landforms: a review of foundation concepts and current understandings. Earth Sci. Rev. 106, 307–331.

Demarchi, L., Bizzi, S., Piégay, H., 2016. Hierarchical object-based mapping of riverscape units and in-stream mesohabitats using LiDAR and VHR imagery. Remote Sens. 8, 97.

Downs, P.W., Dusterhoff, S.R., Sears, W.A., 2013. Reach-scale channel sensitivity to multiple human activities and natural events: Lower Santa Clara River, California, USA. Geomorphology 189, 121–134.

Dufour, S., 2005. Contrôles naturels et anthropiques de la structure et de la dynamique des forêts riveraines des cours d'eau du bassin rhodanien (Ain, Arve, Drôme et Rhône) PhD Thesis Université Jean Moulin Lyon 3, France (244 pp).

Dufour, S., Piégay, H., 2009. From the myth of a lost paradise to targeted river restoration: forget natural references and focus on human benefits. River Res. Appl. 25, 568–581.

Dufour, S., Piégay, H., 2010. Channel vertical mobility, hydro-geomorphic disturbances and understory vegetation in floodplain forests of the Ain River (France). Geomorphologie-Relief Processus Environnement 371–386.

Dufour, S., Rinaldi, M., Piégay, H., Michalon, A., 2015. How do river dynamics and human influences affect the landscape pattern of fluvial corridors? Lessons from the Magra River, Central–Northern Italy. Landsc. Urban Plan. 134, 107–118.

Dunford, R., Michel, K., Gagnage, M., Piégay, H., Tremelo, M.L., 2009. Potential and constraints of unmanned aerial vehicle technology for the characterization of Mediterranean riparian forest. Int. J. Remote Sens. 30, 4915–4935.

Farid, A., Goodrich, D., Sorooshian, S., 2006. Using airborne lidar to discern age classes of cottonwood trees in a riparian area. West. J. Appl. For. 21, 149–158.

Florsheim, J.L., Mount, J.F., Chin, A., 2008. Bank erosion as a desirable attribute of rivers. Bioscience 58, 519–529.

Gagnage, M., 2008. Evaluation des effets des changements morphologiques fluviaux sur la santé des peupliers Master Thesis Université Lumière Lyon 2, France (101 pp).

Geerling, R.A., Ragas, A.M.J., Leuven, R.S.E.W., van den Berg, J., Breedveld, M., Liefhebber, D., Smits, A.J.M., 2006. Succession and rejuvenation in floodplains along the river Allier (France). Hydrobiologia 565, 71–86.

Greco, S.E., Fremier, A.K., Larsen, E.W., Plant, R.E., 2007. A tool for tracking floodplain age land surface patterns on a large meandering river with applications for ecological planning and restoration design. Landsc. Urban Plan. 81, 354–373.

Gurnell, A., 2014. Plants as river system engineers. Earth Surf. Process. Landf. 39, 4–25.

Gurnell, A.M., Petts, G.E., Hannah, D.M., Smith, B.P.G., Edwards, P.J., Kollmann, J., Ward, J.V., Tockner, K., 2001. Riparian vegetation and island formation along the gravel-bed Fiume Tagliamento, Italy. Earth Surf. Process. Landf. 26, 31–62.

Hall, R.K., Watkins, R.L., Heggem, D.T., Jones, K.B., Kaufmann, P.R., Moore, S.B., Gregory, S.J., 2009. Quantifying structural physical habitat attributes using LIDAR and hyperspectral imagery. Environ. Monit. Assess. 159, 63–83.

Hortobágyi, B., Vautier, F., Burkart, A., Wrobel, T.J., Peiry, J.-L., Steiger, J., Corenblit, D., 2015. Use of photogrammetry for the study of riparian vegetation dynamics, I.S. Rivers - 2e Conférence Internationale Recherches et Actions au service des fleuves et grandes rivières (Lyon, France).

Johansen, K., Arroyo, L.A., Armston, J., Phinn, S., Witte, C., 2010. Mapping riparian condition indicators in a sub-tropical savanna environment from discrete return LiDAR data using object-based image analysis. Ecol. Indic. 10, 796–807.

Kondolf, G.M., Piégay, H., Landon, N., 2002. Channel response to increased and decreased bedload supply from land use change: contrasts between two catchments. Geomorphology 45, 35–51.

Kondolf, G.M., Piégay, H., Landon, N., 2007. Changes in the riparian zone of the lower Eygues River, France, since 1830. Landsc. Ecol. 22, 367–384.

Landon, N., Piégay, H., Bravard, J.P., 1998. The Drôme river incision (France): from assessment to management. Landsc. Urban Plan. 43, 119–131.

Lebart, L., Morineau, A., Piron, M., 1995. Statistique exploratoire multidimensionnelle. Dunod, Paris.

Liébault, F., 2003. Les rivières torrentielles des montagnes drômoises: évolution contemporaine et fonctionnement géomorphologique actuel (massif du Diois et de Baronnies) PhD Thesis Université Lumière Lyon II, France (358 pp).
Liébault, F., Piégay, H., 2002. Causes of 20th century channel narrowing in mountain and piedmont rivers of southeastern France. Earth Surf. Process. Landf. 27, 425–444.
Liébault, F., Gomez, B., Page, M., Marden, M., Peacock, D., Richard, D., Trotter, C.M., 2005. Land-use change, sediment production and channel response in upland regions. River Res. Appl. 21, 739–756.
Liébault, F., Piégay, H., Frey, P., Landon, N., 2008. Tributaries and the Management of Main-stem Geomorphology, River Confluences, Tributaries and the Fluvial Network. John Wiley & Sons, Ltd, pp. 243–270.
Liébault, F., Lallias-Tacon, S., Cassel, M., Talaska, N., 2013. Long profile responses of alpine braided rivers in SE France. River Res. Appl. 29, 1253–1266.
Marston, R.A., Girel, J., Pautou, G., Piégay, H., Bravard, J.P., Arneson, C., 1995. Channel metamorphosis, floodplain disturbance, and vegetation development - Ain River, France. Geomorphology 13, 121–131.
Michez, A., Piégay, H., Toromanoff, F., Brogna, D., Bonnet, S., Lejeune, P., Claessens, H., 2013. LiDAR derived ecological integrity indicators for riparian zones: application to the Houille river in Southern Belgium/Northern France. Ecol. Indic. 34, 627–640.
Miller, J.R., Schulz, T.T., Hobbs, N.T., Wilson, K.R., Schrupp, D.L., Baker, W.L., 1995. Changes in the landscape structure of a southeastern Wyoming riparian zone following shifts in stream dynamics. Biol. Conserv. 72, 371–379.
Navratil, O., Legout, C., Gateuille, D., Esteves, M., Liébault, F., 2010. Assessment of intermediate fine sediment storage in a braided river reach (southern French Prealps). Hydrol. Process. 24, 1318–1332.
Ollero, A., 2010. Channel changes and floodplain management in the meandering middle Ebro River, Spain. Geomorphology 117, 247–260.
Pautou, G., Girel, J., 1986. La végétation de la basse vallée de l'Ain: organisation et évolution. Document de Cartographie Ecologique 29, 75–96.
Picco, L., Mao, L., Rainato, R., Lenzi, M.A., 2014. Medium-term fluvial island evolution in a disturbed gravel-bed river (Piave River, Northeastern Italian Alps). Geografiska Annaler Series a-Physical Geography 96, 83–97.
Piégay, H., Landon, N., 1997. Promoting ecological management of riparian forests on the Drôme River, France. Aquat. Conserv. Mar. Freshw. Ecosyst. 7, 287–304.
Piégay, H., Alber, A., Slater, L., Bourdin, L., 2009. Census and typology of braided rivers in the French Alps. Aquat. Sci. 71, 371–388.
Räpple B. Piégay H. Stella J.C. Mercier D. What drives riparian vegetation establishment in river channels at patch to corridor scales? Insights from annual airborne surveys (Drôme River, SE France) (2005 − 2011) (in press).
Segura-Beltrán, F., Sanchis-Ibor, C., 2013. Assessment of channel changes in a Mediterranean ephemeral stream since the early twentieth century. The Rambla de Cervera, eastern Spain. Geomorphology 201, 199–214.
Singer, M.B., Sargeant, C.I., Piégay, H., Riquier, J., Wilson, R.J.S., Evans, C.M., 2014. Floodplain ecohydrology: climatic, anthropogenic, and local physical controls on partitioning of water sources to riparian trees. Water Resour. Res. 50, 4490–4513.
Stella, J.C., Riddle, J., Piégay, H., Gagnage, M., Tremelo, M.L., 2013. Climate and local geomorphic interactions drive patterns of riparian forest decline along a Mediterranean Basin river. Geomorphology 202, 101–114.
Surian, N., 2009. Effects of Human Impact on Braided River Morphology: Examples From Northern Italy, Braided Rivers. Blackwell Publishing Ltd., pp. 327–338.
Taillefumier, F., Piégay, H., 2003. Contemporary land use changes in prealpine Mediterranean mountains: a multivariate GIS-based approach applied to two municipalities in the Southern French Prealps. Catena 51, 267–296.
Toone, J., Rice, S.P., Piégay, H., 2014. Spatial discontinuity and temporal evolution of channel morphology along a mixed bedrock-alluvial river, upper Drôme River, southeast France: contingent responses to external and internal controls. Geomorphology 205, 5–16.
Vallauri, D., Vincent, P., 1999. Histoire de l'occupation de l'espace au XIXème siècle dans les bassins expérimentaux du Saignon, du Brusquet et du Laval (Alpes-de-Haute-Provence). In: Mathys, N. (Ed.), Les bassin versants expérimentaux de Draix, laboratoire d'étude de l'érosion en montagne - actes du colloque "Draix, Le Brusquet, Digne", 22–24 octobre 1997. Cemagref éditions, Antony, pp. 263–277.
Wallick, J.R., Grant, G.E., Lancaster, S.T., Bolte, J.P., Denlinger, R.P., 2008. Patterns and Controls on Historical Channel Change in the Willamette River, Oregon, USA, Large Rivers. John Wiley & Sons, Ltd, pp. 491–516.
Zanoni, L., Gurnell, A., Drake, N., Surian, N., 2008. Island dynamics in a braided river from analysis of historical maps and air photographs. River Res. Appl. 24, 1141–1159.
Ziliani, L., Surian, N., 2012. Evolutionary trajectory of channel morphology and controlling factors in a large gravel-bed river. Geomorphology 173, 104–117.